To the Graduate Council:
I am submitting herewith a thesis written by Donald Doyle entitled "Composite Inert Matrix Fuel Forms in High-Temperature Gas Cooled Micro-Reactors to Reduce Spent Nuclear Fuel, High Level Waste and Environmental Impact." I have examined the final electronic copy of this thesis for form and content and recommend that it be accepted in partial fulfillment of the requirements for the degree of Master of Science, with a major in Nuclear Engineering.

Nicholas R. Brown, Major Professor

We have read this thesis
and recommend its acceptance:

Philip Rack

Lawrence Heilbronn

Accepted for the Council:

Dixie L. Thompson

Vice Provost and Dean of the Graduate School

(Original signatures are on file with official student records.)

Composite Inert Matrix Fuel Forms in High-Temperature Gas Cooled Micro-Reactors to Reduce Spent Nuclear Fuel, High Level Waste and Environmental Impact

A Thesis Presented for the

Master of Science

Degree

The University of Tennessee, Knoxville

Donald Doyle

December 2024

"Oh, the depth of the riches and wisdom and knowledge of God! How unsearchable are his judgments and how inscrutable his ways!

'For who has known the mind of the Lord, or who has been his counselor?'

'Or who has given a gift to him

that he might be repaid?'

For from him and through him and to him are all things. To him be glory forever. Amen."

Romans 11: 33-36 ESV

Acknowledgements

I would like to thank Prof. Nicholas R. Brown for his mentorship and guidance. I thank my committee, Profs. Lawrence Heilbronn and Philip Rack for their feedback. Thanks to Dr. Edward Duchnowski for providing Serpent models of mHTGRs used in this work, the development of the optimization sweeps methodology, and collaboration and feedback throughout the completion of this work. Thanks to Annie Berens and Venkata Vallabhaneni for their collaboration and feedback on this work. Dr. Jason Trelewicz and Dr. Lance Snead of Stony Brook University for their collaboration and material science expertise and input.

I am personally grateful to my friends and mentors, Slade and Julie Griffin, Charles and Robin Robinson, Philip and Karen Rack, and Brandon and Kelly LeMarr, for their continuous support and dedication to pointing me to Christ.

Finally, I would like to thank God, who has given me more grace every day and through whom all things are made possible; all glory be to God.

This work was funded by the DOE ARPA-E grant DE-AR0001620 project MATRICY: Matrix Engineered TRISO Compacts Enabling Advanced Reactor Fuel Cycles.

Portions of this thesis were published in the following peer-reviewed journal article: Donald L. Doyle, Edward M. Duchnowski, Jason R. Trelewicz Nicholas R. Brown. Ceramic composite inert matrix fuel forms in high-temperature gas cooled micro-reactors. Nuclear Science and Engineering, Under review.

Abstract

This work optimizes micro-prismatic high-temperature gas reactor (mHTGR) designs to reduce the energy-normalized mass of spent nuclear fuel and high-level waste (SNF&HLW) produced. The optimization was performed for the current graphite moderator and an inert matrix fuel (IMF) concept employing different composite moderators in a prismatic design architecture. The fuel matrix is magnesium oxide (MgO) with entrained tristructural-isotropic (TRISO) fuel. Moderator material including beryllium oxide (MgO-BeO) and beryllium (MgO-Be) at 40 vol. % loading, and yttrium hydride (MgO-YHx=1.9) and zirconium hydride (MgO-ZrHx=1.9) at 15 vol. % loading were entrained within the MgO host matrix. The optimized designs were evaluated and compared on several fuel cycle metrics.

For the mass of spent nuclear fuel and high level waste per unit of energy generated, the composite moderators saw reductions of between 12.6 and 45.0% compared to the graphite reference case. For the volume of low-level waste (LLW) per unit of energy generated, the composite moderators produced between 31.4 and 43.5% less LLW compared to the graphite reference. The last nuclear waste metric is the energy-normalized mass of depleted uranium per unit of energy generated. The composite moderators continued to perform well compared to the graphite reference case, seeing between 12.6 and 45.0% reduction.

In addition to the nuclear waste metrics, the environmental impact of the reactor fuel

cycles was evaluated by calculating the energy-normalized mass of natural uranium, the mass of carbon dioxide, the land area, and the volume of water used. Overall the composite moderators produced good reductions in the environmental impact of the fuel cycles. The composite moderator's designs did not result in significant increases in the activity of the SNF&HLW after 100 to 100,000 years after reactor shutdown. Compared to a graphite reference, composite moderators significantly reduced nuclear waste, environmental impact, and fuel cost. The reduction compared to a graphite reactor makes the mHTGRs an attractive option for micro-reactor designs.

Table of Contents

List of Tables

List of Figures

Chapter 1

Introduction

1.1 Micro-Reactors

Traditionally, nuclear power plants have been made larger over time to compete economically based on scale; the larger the nuclear plant, the more power it can produce and the more money it makes [16]. The drawback to larger reactors is the increased upfront cost of large plant construction. A new option to help advanced nuclear compete is to scale down to smaller reactors. They are known as small modular reactors (SMRs) or, at smaller scales, micro-reactors. SMRs are reactors that produce less than 300 megawatts of electricity (MWe), and micro-reactors are those that produce less than 30 MWe [2]. The advantages of the SMR and micro-reactors come from the smaller size, allowing for less upfront cost of initial construction. Micro-reactors can also be used in industrial applications to provide low-carbon process steam production on-site by being built on the site of existing industry.

One of the most significant potential markets for micro-reactors is deployment in remote communities. In remote communities currently using diesel generators for their electrical power needs, switching to a micro-reactor reduces cost, increases

reliability, and decreases environmental impact [16]. Another option is deploying micro-reactors in growing urban centers in a "just-in-time capacity" [16]. In this method, a new micro-reactor is brought online just as the electricity demand in the area outgrows the current capacity of the local grid. This addition of a new reactor could then be repeated as the area continues to grow. Adding micro-reactors as the area grows instead of building a large nuclear reactor early on reduces the initial capital costs. In many developing regions, building a large nuclear plant that will not be fully utilized for years to come is not financially viable; meanwhile, micro-reactors allow for the spread of capital costs over many years as the reactors are slowly added to the grid.

Another potential advantage of the micro-reactor design is the transportability of the reactors. Figure 1.1 shows a micro-reactor design concept in a standard shipping container. This portability allows for micro-reactors to deploy quickly to restore power in disaster response or allow for factory manufacturing of the reactors and then shipment to the operation site to reduce cost [57]. Manufacturing at a set facility rather than building on site would allow for micro-reactors to have the advantage of modular manufacturing and the associated cost reductions. Having nuclear plants manufactured off-site and on smaller scales would avoid the lengthy timelines and cost of mega-projects seen in large reactor construction [48].

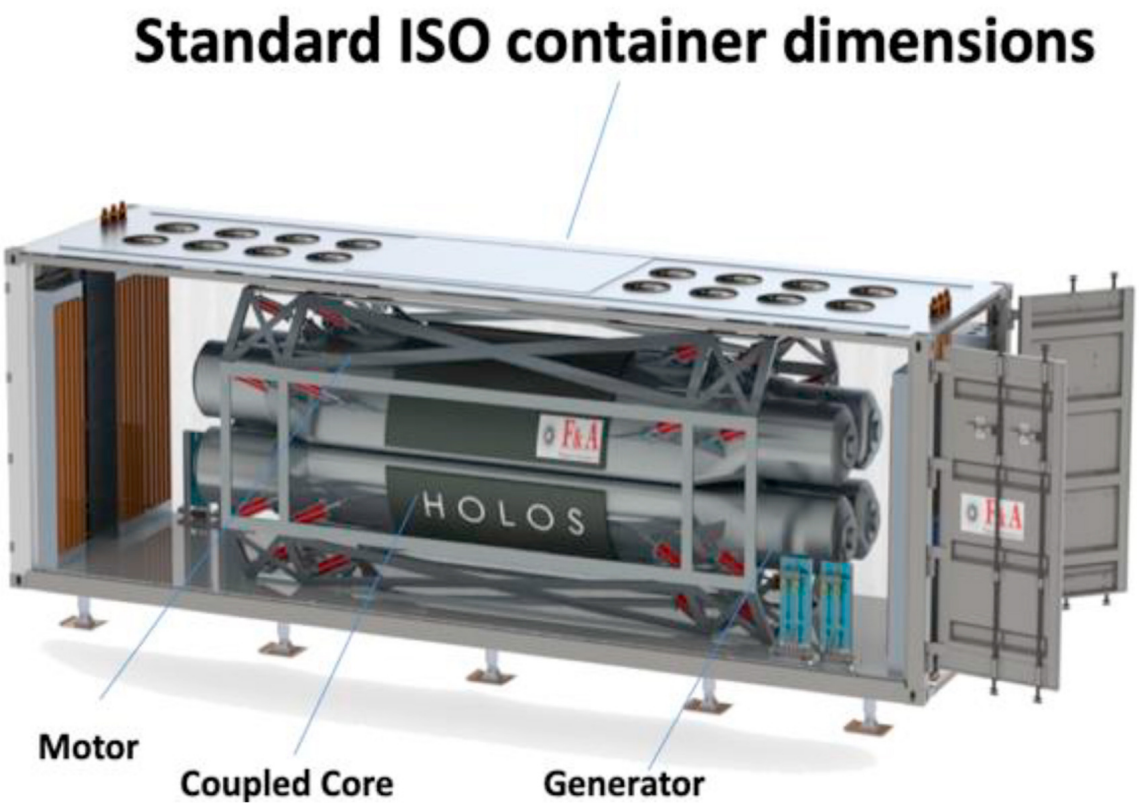

Figure 1.1: Model of a micro-reactor design fitted within a standard shipping container [57]

1.2 High Temperature Gas Cooled Reactors

Micro-reactor designs include designs of several reactor types such as light water, gas-cooled, lead-cooled, molten salt cooled, and sodium-cooled [57][42]. The helium-cooled options known as high-temperature gas-cooled reactors (HTGRs) offer the best option for industrial heat use [42]. Additionally, HTGRs have several passive safety features that make them an appealing option for future nuclear projects. These safety features include negative temperature feedback, ceramic-encapsulated fuel, and passive heat removal [15]. Having negative temperature feedback means that when the reactor core's temperature increases, the reactor's reactivity decreases. Negative temperature reactivity feedback is important as it prevents reactors from melting since decreasing the reactivity will decrease the temperature before the fuel melts. Ceramic encapsulated fuel is a safety feature used to prevent the release of radioactivity into the environment. The fission products are contained within the ceramic fuel matrix; therefore, even if the coolant from the reactor leaks out, there are no radionuclides in the coolant. Having a passive heat removal design prevents nuclear accidents in the case of loss of power. With passive heat removal systems, the heat from the decay heat of the nuclear fuel after a reactor shutdown can be removed without off-site power.

Two primary types of high-temperature gas-cooled reactor designs are prismatic and pebble-beds. Prismatic reactors use prismatic graphite blocks with fuel channels, passing the fuel through the reactor once. Pebble-bed reactor cores comprise pebbles containing the fuel that passes through the core multiple times and offer higher discharge burnup compared to prismatic designs. One of the advantages of HTGRs as an advanced reactor concept is the existence of past experience in the construction and operation of both prismatic and pebble-bed reactors. This experience allows for

lessons learned in the past to be applied to the new designs, offering an advantage over advanced reactor concepts that have never been built before.

The first HTGR built was Dragon, a prismatic design built in the United Kingdom [45]. The reactor was built in 1956 and operated for 12 years. At that time, Dragon faced challenges with heat exchanges and leaks in its helium purification system. Figure 1.2 shows the core configuration of the Dragon reactor. This experience emphasizes the importance of heat exchanger and coolant containment system designs and quality in future reactors. In 1966, the first pebble-bed HTGR went critical in Germany, the "Arbeitsgemeinschaft Versuchsreaktor" (AVR) [45]. The AVR operated for 22 years and produced 15MWe output. The AVR faced issues with the accumulation of graphite dust in the coolant caused by wear on the pebbles as they moved through the core. This challenge could be overcome by considering alternative materials to graphite for the fuel matrix that could better endure the challenges of passing through the reactor core. Peach Bottom I was a 40MWe plant that went critical in 1966 and shut down in 1974 [45]. During its operation, Peach Bottom 1 suffered from several fuel element failures, leading to increased radioactivity in the coolant. The challenge of fuel containment can be addressed through ceramic-encapsulated fuels. The Fort ST. Vrain nuclear reactor was a 330 MWe commercial HTGR located outside Denver, Colorado, and operated commercially from 1979 through 1989 [4]. The Fort ST. Vrain core consisted of hexagonal graphite blocks surrounded by 3 to 4 feet of graphite reflector [26]. Figure 1.3 shows the core configuration of the Fort ST. Vrain reactor [26]. A test pebble-bed small HTGR has been constructed in China, and the HTR-10 Figure 1.4 shows the reactor design [60]. Two transients without SCRAM scenarios were tested with the HTR-10, which demonstrated the passive safety of HTGRs [31]. The higher temperatures that are achieved in HTGRs compared to traditional light water reactors allow HTGRs the

potential to provide process heat for industrial processes [42] [10], [11]. The ability to drive industrial processes allows HTGRs to load follow the grid by integrating with industrial applications when electricity demand is low [47]. This ability to load follow means that HTGRs could integrate with renewable energy sources to provide base load power on demand.

1.3 Environmental Impact

One of the significant driving forces behind the renewed push for nuclear power is the need to reduce the environmental impact of power generation. The drive to reduce climate change has led to numerous countries starting or restating the creation of new nuclear power programs [57]. Studies have found that the use of nuclear power can significantly reduce the production of carbon dioxide in the power generation process [57][3][1][32][41]. Nuclear power is beneficial in reducing the environmental impact through reduced carbon dioxide emissions. Figure 1.5 shows the mass of carbon dioxide produced in tonnes for each gigawatt of electricity generated for the various electricity-producing options. As can be seen, nuclear energy is among the lowest producers of carbon dioxide, along with hydroelectric, wind, and biomass options. Another consideration in the environmental impact of electricity generation is land use. Figure 1.6 shows the land area used per unit of energy generated for several electricity-producing options. The data shows that nuclear has the second lowest footprint of any power-generating option behind natural gas [58]. Between Figures 1.5 and 1.6, it is seen that nuclear power has the lowest overall environmental impact when considering both carbon dioxide emissions and land area use. Overall, nuclear power is recognized as a critical part of clean energy development [46].

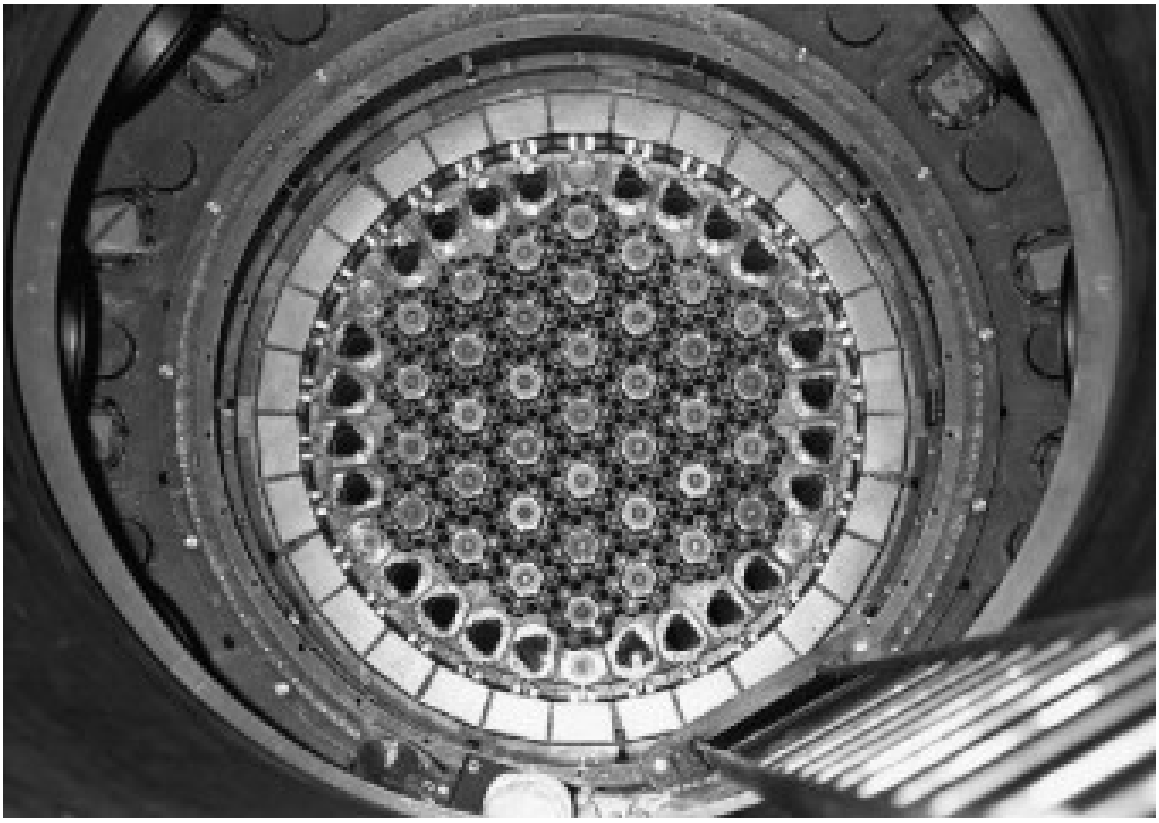

Figure 1.2: The core of the Dragon nuclear reactor loaded with dummy fuel elements [43]

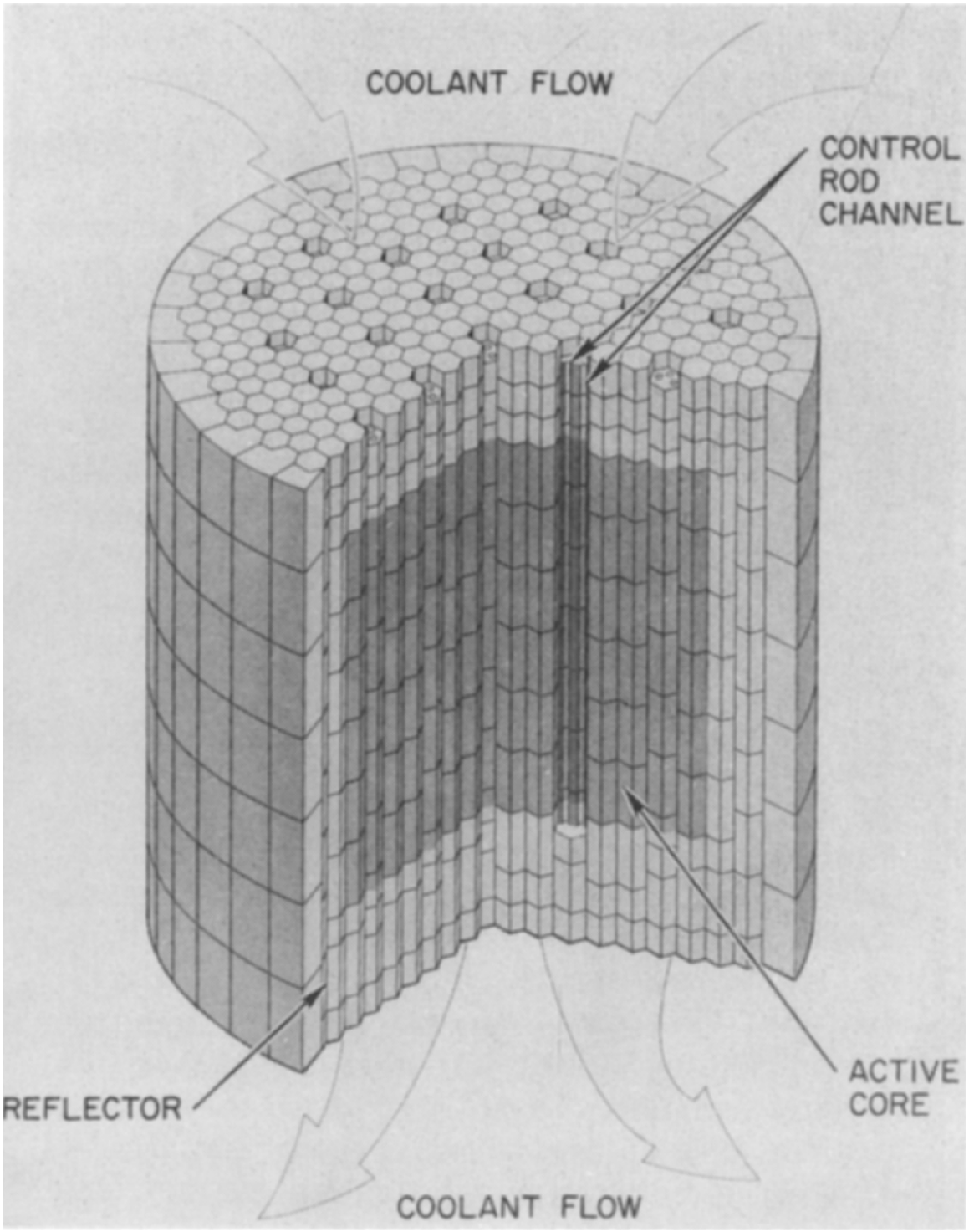

Figure 1.3: Core configuration of the Fort ST. Vrain nuclear reactor [26]

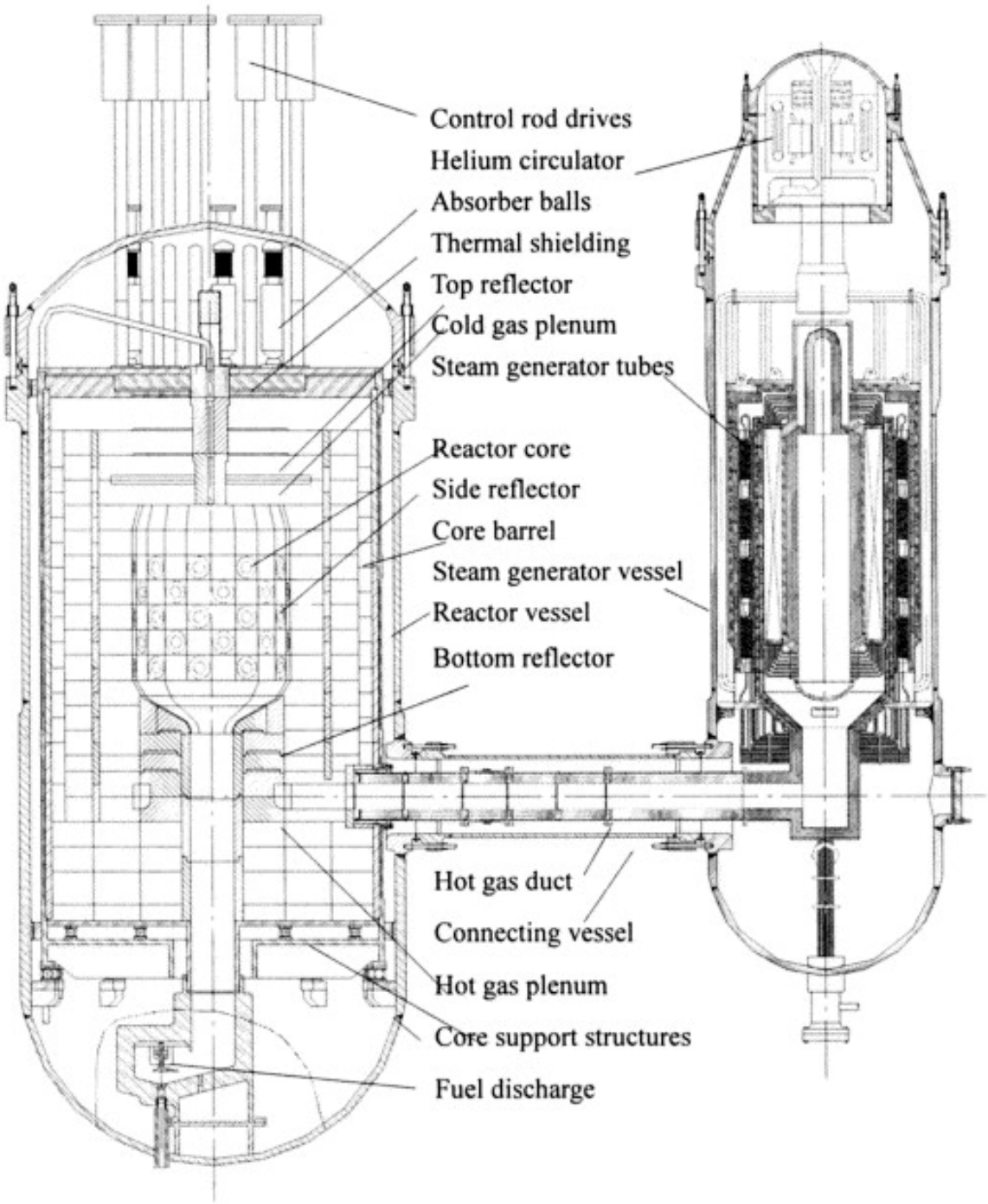

Figure 1.4: HTR-10 reactor design [60]

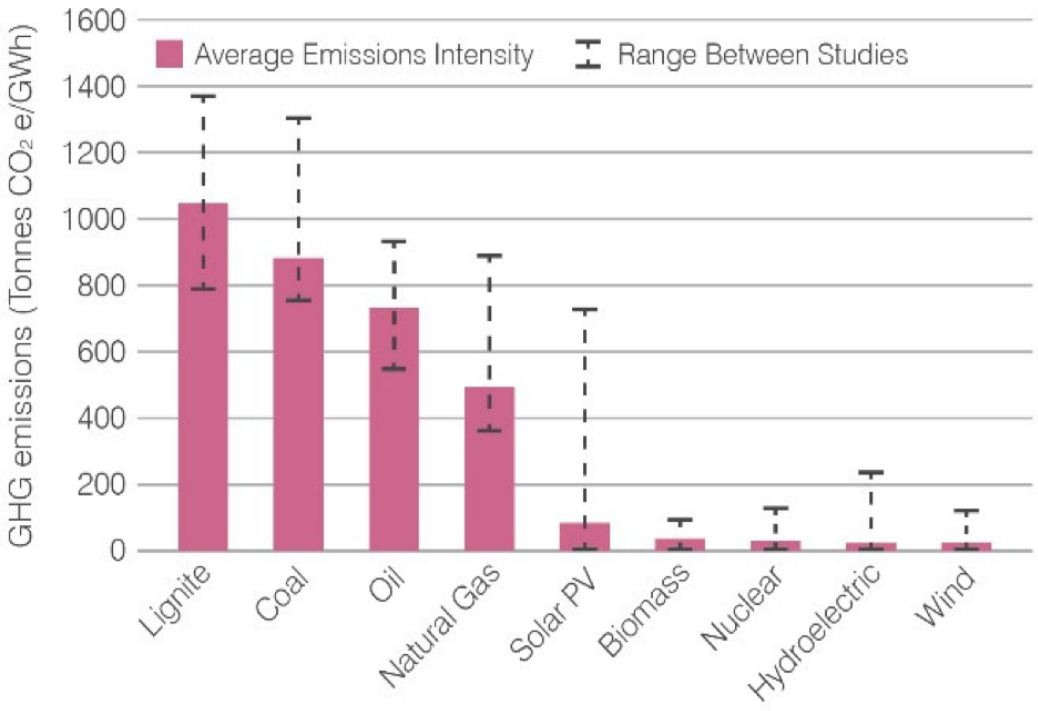

Figure 1.5: Comparison of carbon dioxide produced per unit of energy generated for various electricity producing options [46]

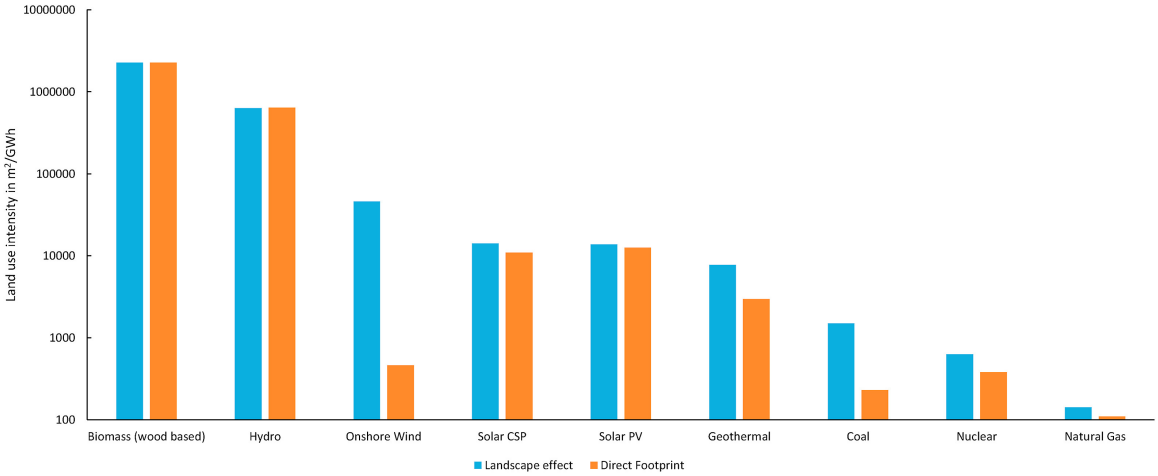

Figure 1.6: Comparison of the land area used per gigawatt hour of electricity produces for various electricity producing options [58]

Another by-product of nuclear power that must be considered is the nuclear waste produced. Nuclear waste is radioactive and must be safely stored for long periods to protect it from contamination [36]. As of 2017, the United States had 79000 metric tons of spent nuclear fuel and high-level waste [59]. The concerns and cost of disposal and protection of spent nuclear fuel and high-level waste are another hindrance to constructing new nuclear power. While permanent solutions such as a geological repository will be necessary, reducing the mass of waste produced per unit of energy generated will reduce the stain of disposal [36].

1.4 Nuclear Fuel

The fuel used in HTGRs provides one of the main safety features of the design. HTGRs use tristructural-isotropic (TRISO) fuel, a ceramic-encapsulated fuel that retains fission products within the fuel pellet. Past HTGRs that have been built used various forms of encapsulated fuel. The Dragon reactor in the United Kingdom used an encapsulated fuel with a pyrolytic carbon coating over the fuel and several experimental coatings over the reactor lifetime [43]. Peach Bottom 1 used a pyrolytic carbon-coated fuel in the first fuel loading [25]. In subsequent loading, Peach Bottom 1 used BISO fuel [22]. BISO fuel includes a low-density buffer layer and an outer pyrolytic carbon coating. The AVR reactor was initially also loaded with BISO particles but was later updated to use TRISO particles [20]. The Fort ST. Vrain reactor used an early form of encapsulated fuel with pyrolytic carbon and silicon carbide layers [26]. The HTR-10 in China employs UO2 TRISO, as does the larger HTR-PM [60] [37].

In TRISO fuel, the fuel kernel is coated in a low-density graphite buffer layer followed by a pyrolytic carbon layer, a silicon carbide layer (SiC), and another pyrolytic carbon

layer [7]. The low-density buffer layer in the TRISO protects the outer layers from pressure due to fission gas release and fuel swelling [53]. The inner pyrolytic carbon layer protects the fuel kernel from interactions with the SiC layer and contains the gaseous fission products. [20]. The SiC is the primary retention method of non-gaseous fission products and provides strength to the fuel pellet. The outer pyrolytic carbon layer offers another barrier against gaseous fission product release. The multiple layers act together to provide a robust defense against fission product release [24]. Figure 1.7 shows a cross-section of a UCO TRISO particle with each layer labeled. TRISO fuel forms have been considered for prismatic and pebble-bed HTGR designs and other reactor concepts, including light water and molten salt-cooled reactors [7]. Figure 1.8 shows fueling a pebble-bed and prismatic fuel element with TRISO particles. For the pebble-bed HTGR, the TRISO particles are encased in the pebbles, and then the pebbles are loaded into the reactor core. In the case of a prismatic HTGR, the TRISO is loaded into fuel elements that are, in turn, loaded into the prismatic blocks that form the reactor core. The central fuel kernel in TRISO fuel for HTGRs has been UO2; however, due to the corrosion caused by CO produced from excess O, the use of UCO uranium fuel kernels has been proposed [40]. Light water reactors (LWR) offer one potential design type that could benefit from TRISO fuel's advanced safety benefits. However, the UO2 and UCO TRISO particles do not provide sufficient fuel loading for LWRs [23]. As a solution to the limited fuel loading, a UN-based TRISO kernel was developed with a higher uranium density and larger diameter than UCO TRISO [56]. Figure 1.9 shows a UN TRISO particle compared with the UCO TRIO in Figure 1.7. The size difference is clear, with the UN TRISO being more extensive and containing more fuel. The UN TRISO also has a higher uranium density because the UN has one uranium per nitrogen atom, while UCO has one uranium per 2 carbon or oxygen atoms. This higher density further increases

the additional uranium in UN TRISO over UCO TRISO. While initially proposed for LWR use, the higher uranium mass achievable using UN TRISO is favorable for smaller nuclear reactors to increase fuel loading. For this reason, UN fuel is considered in this work as the fuel for micro-HTGRs as it allows for higher burnup in a smaller core configuration.

1.5 Composite Moderators

Conventionally, the TRISO particles in HTGRs have been contained in a graphite matrix in both prismatic and pebble-bed designs [26] [60] [37]. The safety of the reactors can be improved with the use of a ceramic such as silicon carbide (SiC) to encase the TRISO particles, forming a fully ceramic encapsulated (FCM) fuel form; this addition of another barrier to fission product release [56], [54] [38]. The use of FCM fuel, as with the UN fuel, was a development made towards improving safety in LWRs. As with the UN TRISO particles, the same benefits can be leveraged to enhance HTGR design's safety features [39]. One of the current limitations of HTGRs is the volume change of graphite under high-temperature irradiation; the graphite initially shrinks and then experiences turnaround and swells. The initial shrinkage and final swelling can result in up to an 8% change in original volume [13], [50]. In addition to volumetric changes, the thermophysical properties of graphite also change under irradiation, particularly when irradiated at high temperatures [49], [35], [28]. This instability under irradiation can impose lifetime limits on reactor cores dictated by the graphite damage levels. The SiC employed in FCM exhibits better radiation stability with less than a 2% volume change at relevant operating temperatures [55], [44], [51].

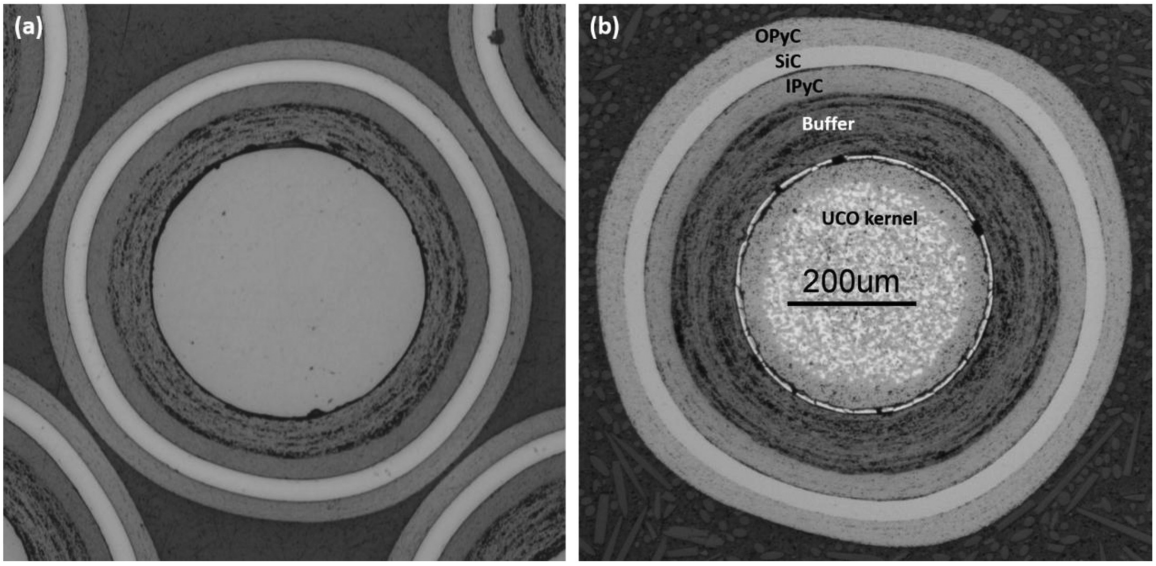

Figure 1.7: Layers in a TRISO particle [20]

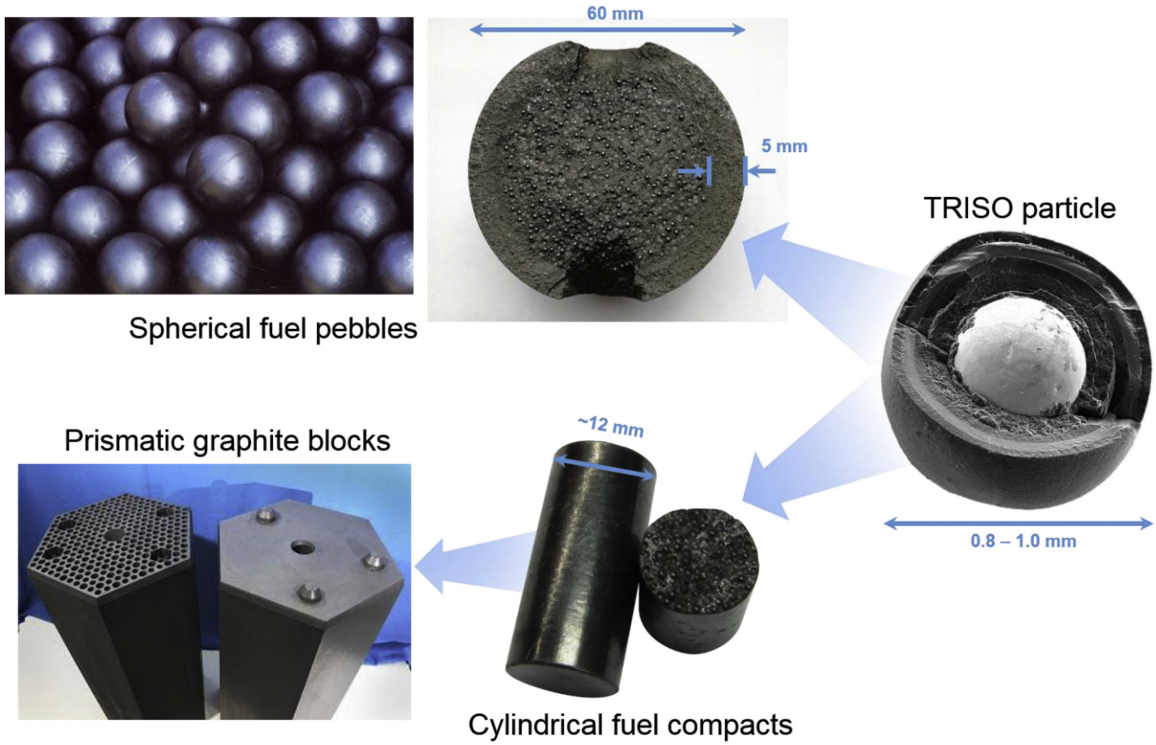

Figure 1.8: The use of TRISO fuel in both pebble-bed and prismatic reactors [20]

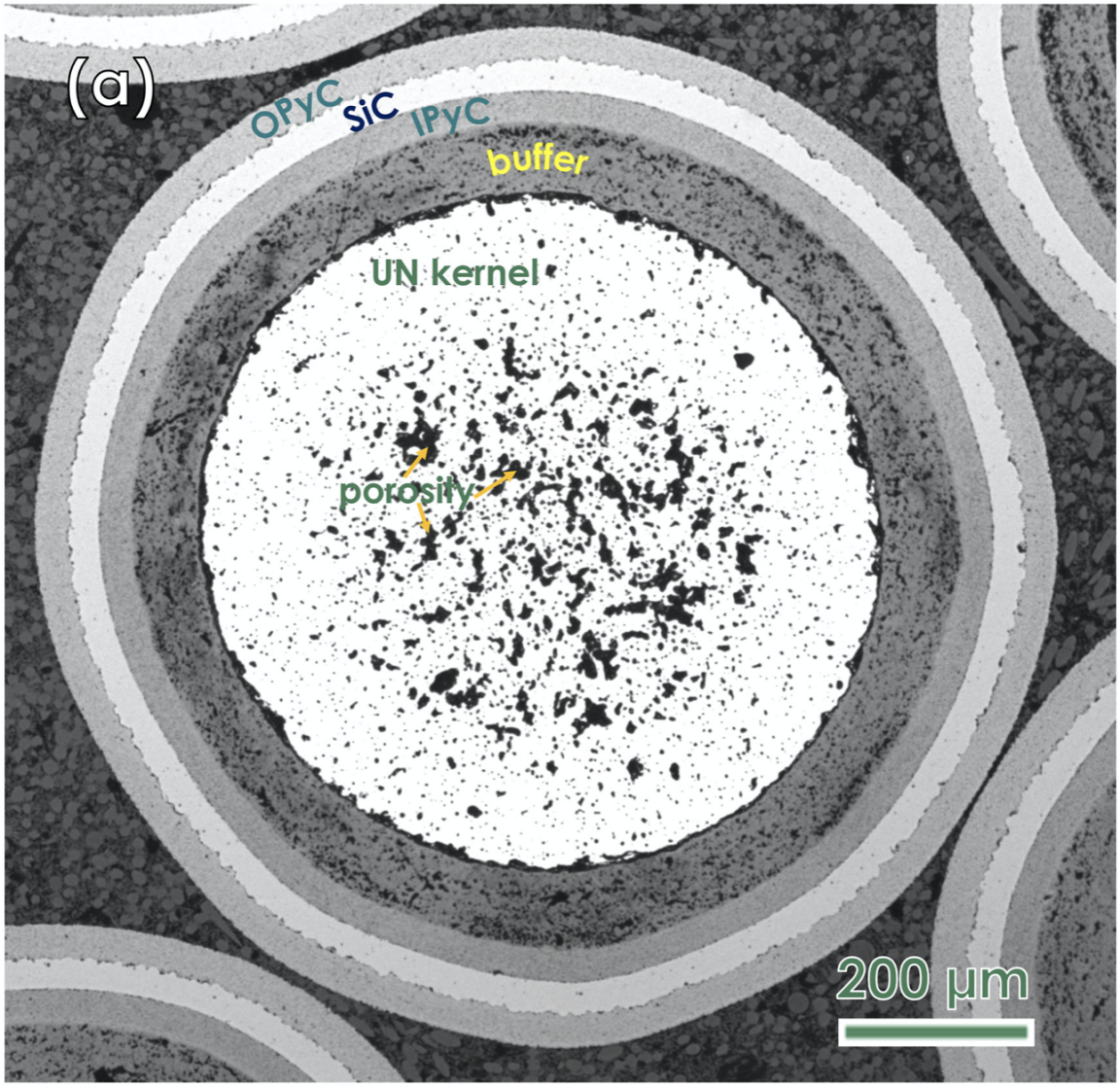

Figure 1.9: Uranium nitrite TRISO particle [56]

A drawback to FCM fuel is that adding SiC to the fuel matrix reduces the moderating power and, in turn, the discharge burnup and fuel utilization, resulting in increased environmental impact [39]. // While FCM fuel using SiC has safety advantages, an inert matrix fuel form (IMF) concept with improved moderating power offers increased discharge burnups in addition to enhanced safety. Ceramic-composite IMF technologies offer one solution to balancing irradiation stability with moderating power by training a strong moderating material within an irradiation-stable host matrix [52]. Figure 1.10 shows the composite moderator concept and the advantages of each material being used. The host matrix provides stability, strength, and heat conduction, while the entrained phase provides high moderation. The use of composite moderators in HTGR applications has been previously studied and found to improve reactor performance metrics compared to traditional graphite reactors [34], [18], [21]. For the moderating phase, four materials have been studied: beryllium (Be), beryllium oxide (BeO), yttrium hydride (YHx=1.9), and zirconium hydride (ZrHx=1.6). While the monolithic versions of these materials offer high moderation, none intrinsically have the temperature and irradiation stability to be fielded in an HTGR [18]. Magnesium oxide (MgO) has previously been selected as an irradiation-stable matrix material [17], [19] and builds on past works [18], [21] to leverage the composite moderators and UN TRISO IMF technologies to optimize micro-HTGR performance.

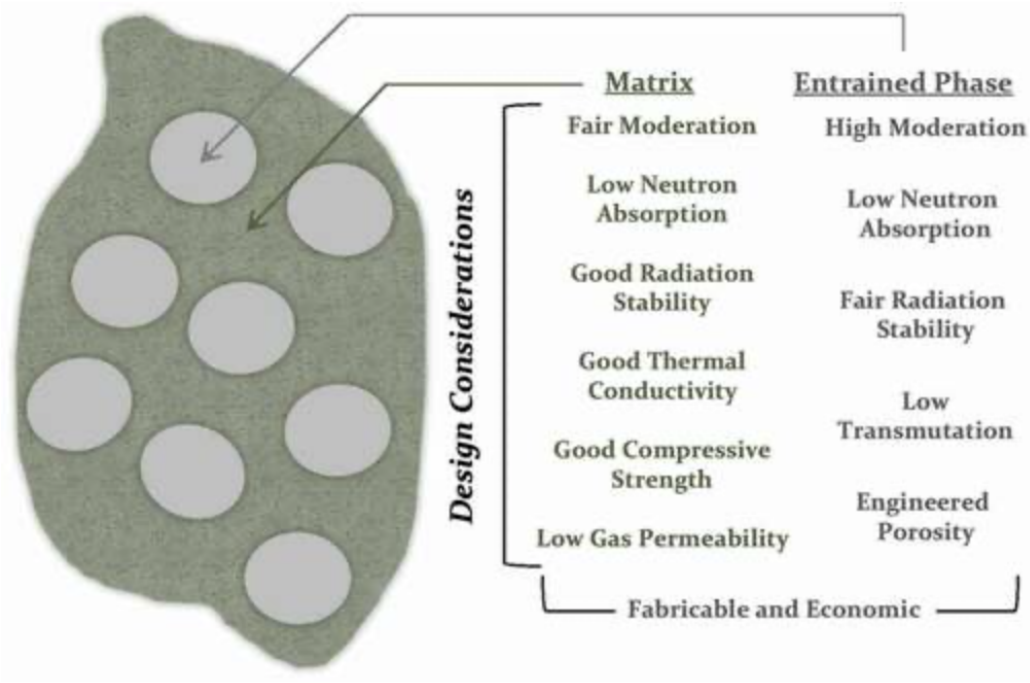

Figure 1.10: Composite moderator concept [52]

Chapter 2

Methods

This work found optimal configurations of mHTGRs using the current state-of-the-art graphite moderator material and four composite moderator materials. The fuel-to-moderator ratio was adjusted to achieve the highest discharge burnup in each case. The mass of nuclear waste, fuel cost, and environmental impact were evaluated to evaluate the benefits of composite moderators in mHTGR designs. Each metric was then compared between the composite moderator designs, the current state-of-the-art graphite mHTGR design, and a light water SMR and LWR from the literature. The evaluation methods from the DOE-NE Fuel Cycle Evaluation and Screening (E&S) study were used to calculate the mass of nuclear waste, fuel cost, and environmental impact per unit of electrical energy produced [33]. The evaluation methods used energy to normalize all metrics to provide a one-to-one comparison across reactor concepts and sizes. The methods from the E&S study have been used as a basis to evaluate: LWRs with fuel enriched over 5% [14], SMRs [6], [12], [29], externally driven thorium [9] or uranium [27] based systems, intermediate neutron spectrum systems for continuous thorium recycling [5], micro-heat pip cooled reactors [30], the use of TRISO fuel in LWRs [8]. Based on the wide use in literature across multiple reactor

concepts and proposed fuel cycles, the E&S metrics provide a basis for evaluating and comparing fuel cycles. This work uses the E&S metrics to evaluate the optimized micro-HTGR designs by comparing the optimized graphite reference HTGR, current LWR, and SMR data metrics against the four composite moderator IMF designs. Figure 2.3 shows the fuel cycle that the studied reactors use, a once-through uranium fuel cycle in an HTGR.

2.1 Reactor Design Development

Prismatic micro-HTGR designs were considered in this work using several moderator concepts and inert matrix fuel (IMF) forms. The size constraints were set to be 90cm in radius to the outer reflector and a height of 395.5cm as used in [21] and inspired by the Project Pele constraints. The power was set to 10MWth to match the power of the HTR-10 [26].

A reference design was developed and evaluated to compare the new composite moderator designs. The reference design is a prismatic micro-HTGR fueled by 19.9% enriched UCO TRISO. The radius and densities of the UCO TRISO can be seen in Table 2.1. The TRISO used in the two-phase composite moderator designs was a 19.9% enriched UN fuel. The radius and densities of the TRISO layers are shown in Table 2.2. The radii of the TRISO particles were the same for both designs to keep constant geometric constraints. Compared to the UCO TRISO, according to the reference design, the UN TRISO has a higher fuel density. The higher density and higher atom density of uranium in UN compared to UCO combine for a higher fuel mass in the advanced reactors TRISO particles.

Table 2.1: UCO TRISO layer radii and densities [21]

Layer	Radius [cm]	Density [g/cc]
UCO kernel	0.0425	10.9
Buffer	0.0475	1.0
PyC layer	0.0510	1.90
SiC layer	0.0545	3.20
PyC layer	0.0580	1.90

Table 2.2: UN TRISO layer radii and densities [55]

Layer	Radius [cm]	Density [g/cc]
UCO kernel	0.0425	14.3
Buffer	0.0475	1.0
PyC layer	0.0510	1.90
SiC layer	0.0545	3.20
PyC layer	0.0580	1.90

The IMF fuel consists of the UN TRISO entrained within a MgO ceramic matrix. This fuel is surrounded by composite moderators in a prismatic architecture, with the cross-section in Figure 2.1 illustrating the relative locations of the IMF and moderators. Four entrained moderating materials were evaluated in this study as described in Table 2.3, and reactor designs were optimized to maximize the discharge burnup of the nuclear fuel. The micro-HTGR designs are based on previous work looking at advanced moderator concepts [21]. Figure 2.2 shows the reactor geometry, a radial slice (left), an axial slice (center), and fuel assembly (right). The same designs from the previous work were used as a starting point and optimized for discharge burnup. The discharge burnup was optimized by changing the lattice pitch and TRISO packing fraction to change the fuel-to-moderator ratio within the reactor core. In this optimization process, the reactors were simulated in the Monte Carlo neutronic code Serpent, a 3D continuous-energy Monte Carlo reactor physics burnup calculation code using ENDF/B-VII.1 cross-sections. The reactors were then depleted to subcritical, and the discharge burnup was calculated for when reactivity reached zero. Simulations were run with lattice pitches of 2.0, 2.2, 2.4, and 2.5cm and for TRISO packing fractions between 5 and 50% at increments of 5% for each lattice pitch. This optimization was independently performed for the four IMF concepts and the graphite reference. In total, 200 reactor designs were evaluated using Serpent. Based on the results of the optimization study, an optimal core configuration was selected for each IMF concept based on producing the highest discharge burnup. Evaluation metrics were then calculated for the optimal configurations for the IMF concepts and the reference graphite design. The evaluation metrics were then compared between the IMF concepts and the graphite reference designs, a light water small modular reactor (SMR) and a traditional large light water reactor (LWR).

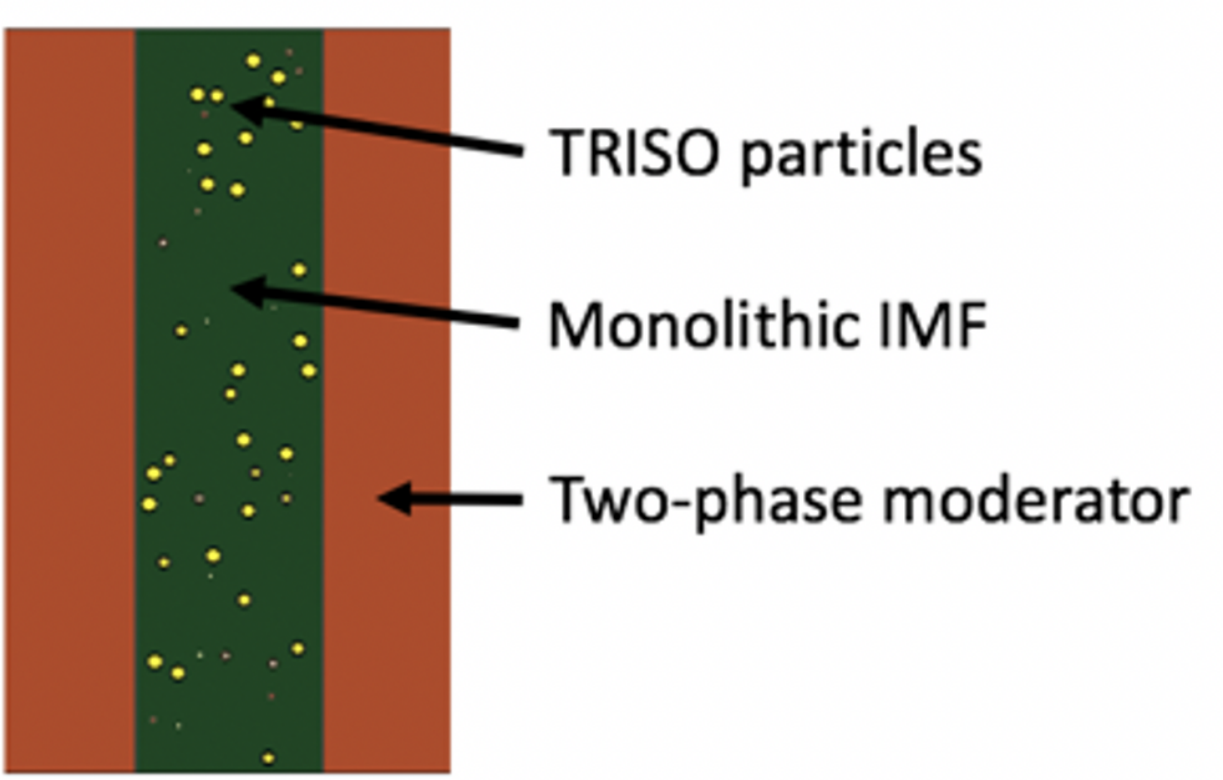

Figure 2.1: IMF within a prismatic reactor platform

Table 2.3: Two-phase composite moderator materials and volume percent [21]

Composite Moderator	Host Material	Moderator Material
$MgO - Be$	$MgO60\%$	$Be40\%$
$MgO - BeO$	$MgO60\%$	$BeO40\%$
$MgO - YH1.9$	$MgO85\%$	$YH1.915\%$
$MgO - ZrH1.6$	$MgO85\%$	$ZrH1.615\%$

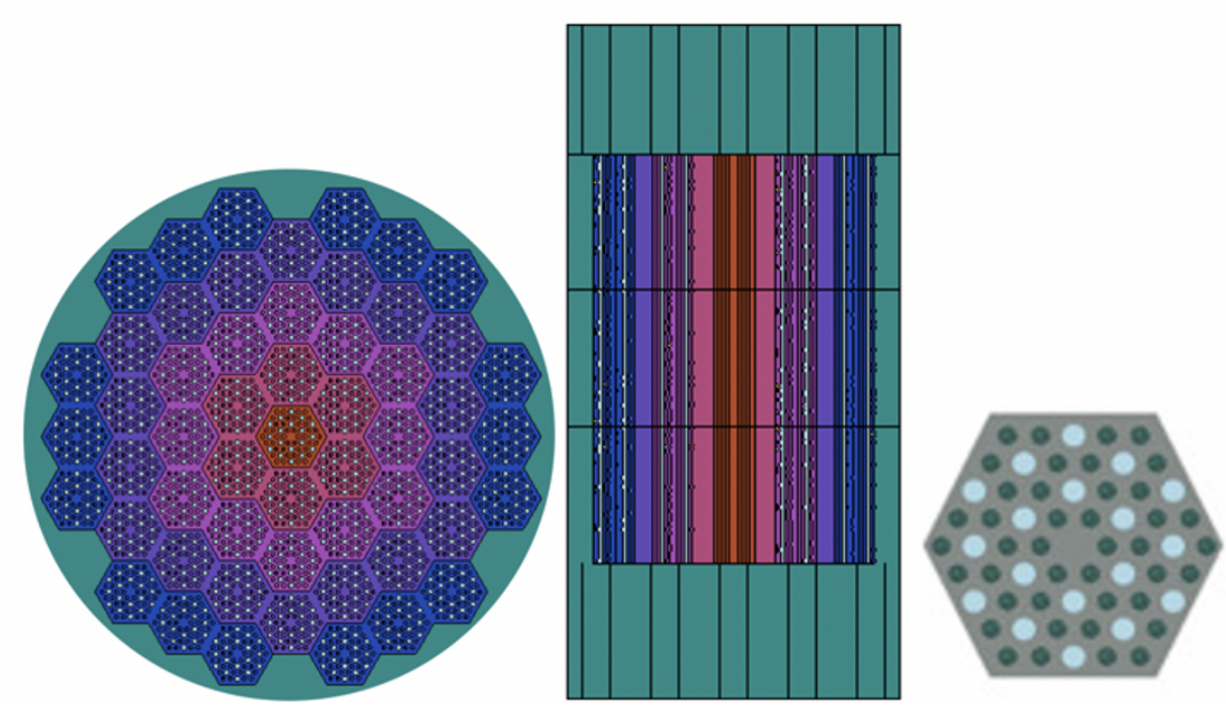

Figure 2.2: Radial (left) and axial (middle) crosscut of the prismatic microreactor. Prismatic microreactor assembly (right) [21]

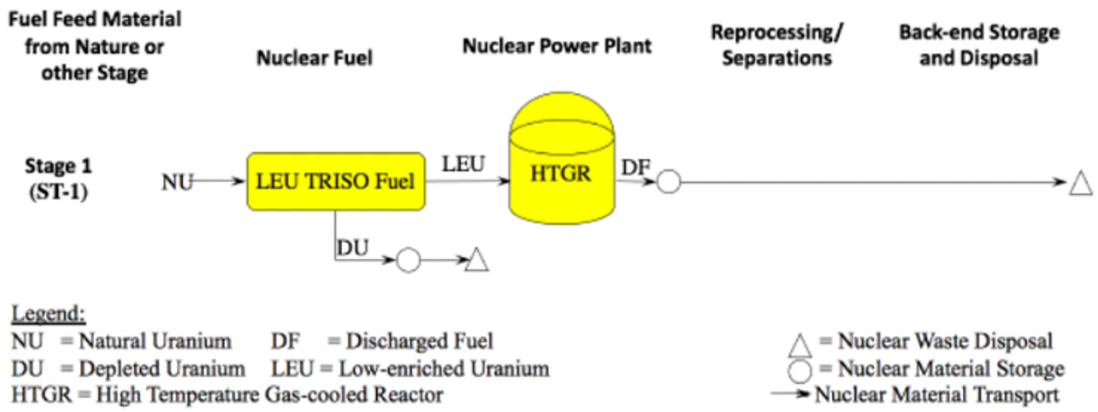

Figure 2.3: Once-through fuel cycle diagram (EG02). Reproduced from the E&S study [33]

2.2 Waste Metric Calculations

Equation 2.1 calculates the mass of SNF&HLW. The SNF&HLW includes the heavy metal and fission products from the initial fuel mass but does not include any structural materials [33]. The mass of SNF&HLW depends only on the fuel discharge burnup and the thermal-to-electrical efficiency of the reactor designs. In Equation 2.1: DB is the discharge burnup, and ϵ is the thermal to electrical efficiency of the reactor, assumed to be 0.5 for the HTGRs.

$$M_{SNF\&HLW}[MTHM/GWe-y] = \frac{1}{DB * \frac{1}{365.25}\epsilon} \tag{2.1}$$

Several intermediate values are needed to calculate the metrics to evaluate the reactor, the mass of fuel moving through the fuel cycle (M_f), the number of separative work units (SWU) needed for enrichment, the equation to calculate SWU needs the result of the value function (V(wt%)) for the fuel, natural and depleted uranium enrichment percentages. Equation 2.2 is used to calculate the energy normalized mass flow based on the thermal power of the reactor ($P_{thermal}$), the electrical power of the reactor ($P_{electirc}$), and the discharge burnup of the fuel (DB). The SWU is calculated using Equation 2.1 based on the energy normalized mass of fuel, depleted, and natural uranium: (M_f, M_{DU}, and M_{nat}), and results of the value function for their respective enrichment's. The value function is shown in Equation **??** and depends only on the weight percent enrichment of U-235 for the evaluated design.

$$M_f = P_{thermal}/(P_{electirc} * DB) \tag{2.2}$$

$$SWU[kSWU/GWe-y] = M_f V_f(F_{en}) + M_{DU} V_f(D_{en}) - M_{NAT} V_f(N_{en}) \tag{2.3}$$

$$V(wt\%) = (1-2*wt\%)*ln((1-wt\%)/(wt\%)) \tag{2.4}$$

The volume of low-level waste (LLW) was calculated for each reactor using Equation 2.5. The C_{enr} and C_{fab} values are multiplier constants for volume LLW produced during the enrichment and fabrication, and C_{rec} is an additive constant of LLW produced during reactor operations. All three metrics are from the evaluation and screening study and are 0.44 [m3/kSWU], 0.945 [m3/tHM], and 261 [m3/GWe-y] for the enrichment, fabrication, and reactor operations stages, respectively [33]. The reactor operation stage produces most of the LLW, including the waste produced during the reactor decommissioning process. This large constant contribution from general operation independent of reactor concepts will result in reduced improvement in this metric due to better fuel utilization having a more limited effect on the overall volume of LLW produced per unit of energy generated. For the graphite reference micro-HTGR, the volume of the moderator graphite material in the fuel assemblies was also considered LLW. The moderator material in the two-phase IMF designs was not considered LLW based on being more stable under neutron irradiation.

$$LLW[m^3/GWe-y] = C_{enr} * SWU + C_{fab} * M_f + C_{rec} \tag{2.5}$$

The mass of depleted uranium is calculated as a separate metric from the SNF&HLW, as its radioactivity does not dictate the same isolation level [33]. The metric is still considered nuclear waste, requiring a disposal path, though it will be unique from the SNF&HLW path. Since no reprocessing is considered in the studied fuel cycles, the mass of depleted uranium is the difference between the natural uranium used and the fuel mass, as shown in Equation 2.6.

$$M_{DU}[MTDU/GWe-y] = M_{NAT} - M_{SNF\&HLW} \tag{2.6}$$

2.3 Environmental Impact Calculations

The mass of natural uranium used by the reactor designs over the fuel cycles was evaluated. The mass of natural uranium is considered elemental uranium and provides a measure of natural resources utilized for each reactor concept [33]. Equation 2.7 shows the equation used to calculate the mass of natural uranium used based on the fuel mass flow and the enrichment of the fuel, tails, and natural uranium: $E_{fuel} = 19.9$, $E_{tails} = 0.25$, and $E_{natural} = 0.711$ weight percent U-235 respectively.

$$M_{NAT}[MTNU/GWe - y] = M_f * \frac{E_{fuel} - E_{tails}}{E_{natural} - E_{tails}} \tag{2.7}$$

The mass of carbon dioxide, the land area, and the water volume are calculated using multipliers for each stage of the fuel cycle, shown in Tables 2.4, 2.5, and 2.6 and taken from the evaluation and screening study [33]. The fuel cycle can be broken into four major stages: the front-end fuel cycle, fuel fabrication, reactor operation, and disposal and transportation. The front end of the fuel cycle includes the mining and milling process, uranium conversion, enrichment, and deconversion. The fuel fabrication is not broken down into sub-processes. The reactor stage includes reactor construction, operation, and waste conditioning processes. The disposal and transportation process includes shallow land burial, geologic repository, interim storage, and waste packages and drip shields processes. Multipliers for each of the environmental impact metrics are included for each applicable stage and sub-process in Tables 2.4, 2.5, and 2.6, not all processes contribute to all metrics. To calculate the total energy normalized value of the metrics, the multipliers at each stage are multiplied with the re-normalization factor relevant to the process as listed in Tables 2.4, 2.5, and 2.6, the re-normalization parameters were calculated using Equation 2.1, Equation 2.2, Equation 2.3, Equation 2.7, and Equation 2.6. The reactor construction

and operations values are independent of fuel cycle choice. They are not multiplied by any re-normalization constant but are given in energy-normalized units and added to the total values.

The mass of carbon dioxide includes carbon dioxide produced from producing the energy used in the fuel cycle and that produced by the manufacturing of materials consumed over the fuel cycle [33]. Examples of carbon dioxide production across the fuel cycle include electricity and heat for operating the non-power plant facilities: fuel fabrication, waste storage facilities, emissions for mining and transportation equipment, and from the concrete used in the construction of the various facilities involved, including the nuclear power plant. Table 2.4 shows the multiplier constants for carbon dioxide. The fuel cycle's mining, milling, and conversion phases have significant carbon dioxide multiplier constants. As both these multipliers are normalized using the mass of natural uranium, the increased enrichment in the HTGR designs leading to increased natural uranium utilization will also increase the carbon dioxide produced over the fuel cycle. The reactor construction also has a large additive constant to the carbon dioxide mass that the IMF reactor designs will not impact. The large quantities of carbon dioxide produced during the fuel fabrication process and in the disposal of SNF&HLW, such as waste conditions, geologic repository, interim storage, waste packages, and drip shields, provide potential benefits from the IMF reactor concepts. The fuel fabrication is re-normalized using the fuel mass flow, and the SNF&HLW disposal multipliers are all re-normalized utilizing the mass of SNF&HLW. Both the total fuel mass and mass of SNF&HLW are expected to be reduced in the IMF reactor designs. Leading to significant reductions in the mass of carbon dioxide produced.

Table 2.4: Multiplier constants for carbon dioxide use calculations [33]

Process	Multiplier	Units
Mining/Milling	$8.3E04$	$kg/MTNU$
Conversion	$2.2E04$	$kg/MTNU$
Enrichment	$2.8E01$	kg/SWU
Deconversion	$-3.2E03$	$kg/MTDU$
Fabrication	$2.85E05$	$kg/MTIHM$
Reactor Operation	$1.16E07$	$kg/GWe-y$
Transports	$1.82E00$	$kg/MTIHM$
Repository Excavation	$2.49E04$	$kg/MRIHM$
Repository Operations	$6.32E04$	$kg/MTIHM$
Waste Fabrication	$2.71E04$	$kg/MTIHM$
Waste Package	$2.91E04$	$kg/MTIHM$
Waste Drip Shield	$1.30E03$	$kg/MTIHM$
Concrete Manufacture	$3.11E04$	$kg/MTIHM$

The land area metric considers the land area utilized across the fuel cycle, including mining, fuel production facilities, reactor sites, exclusion zones, and waste disposal sites [33]. From Table 2.5, the mining and milling, fuel fabrication, reactor operation, and geological repository significantly impact the land area used. The mining and milling process uses a large land area in the mining process, which is lumped with milling since this process generally occurs at the mining site [33]. The fuel fabrication multiplier is based on the land area, lifetime, and annual throughput of the Westinghouse Columbia UOX fuel fabrication plant [33]. The reactor operation term is the largest of the terms for land area, and while it is an additive rather than mutative constant, it will have a notable impact on the land area used. The significant value of land area used in reactor operations is driven by the assumption that the exclusion area is non-recoverable and counted as the area used [33]. Finally, the geological repository impact comes from the need to store the spent fuel in permanent isolation and again accounts for the radiological exclusion zone around the actual repository [33]. When applying these values to the IMF micro-HTGRs in this work, the higher enrichment will increase land area at the mining and milling stage by requiring more natural uranium. This increase will be more than counteracted by the decreased land area at the fuel fabrication and geological repository stages due to high burnups. This reduction leads to less fuel needing to be fabricated and less SNF&HLW production. Table 2.6 shows the multiplier constants for the water volume used at each fuel cycle stage. All multiplier values come from the evaluation and screening study [33]. The multipliers in Table 2.6 show that the reactor operation constant is orders of magnitude greater than any of the other constants. Since the rector operation is an additive constant and is not multiplied by anything over the fuel cycle, the potential impact on water usage is limited to its effect on the other constants.

Table 2.5: Multiplier constants for land use calculations [33]

Process	Multiplier	Units
Mining	$2.8E-04$	$km^2/MTNU$
Conversion	$3.3E-06$	$km^2/MTNU$
Enrichment	$9.0E-09$	km^2/SWU
Deconversion	$9.3E-05$	$km^2/MTDU$
Fabrication	$1.02E-04$	$km^2/MTIHM$
Reactor Operation	$7.27E-02$	$km^2/GWe-y$
Waste conditioning	$4.41E-05$	$km^2/MTIHM$
Land Burial	$9.74E-06$	$km^2/MTDU$
Repository	$1.5*E-03$	$km^2/MTIHM$
Interim	$3.0*E-05$	$km^2/MTIHM$

Since the rector operation is an additive constant and is not multiplied by anything over the fuel cycle, the potential impact on water usage is limited to its effect on the other constants. Due to the large discrepancy in magnitude, the volume of water used per unit of energy generated is almost entirely constant across all reactor designs. The significance of the reactor operation phase comes from water being used as the ultimate heat sink. In the power generating loop of a nuclear reactor plant, water is boiled, run through a steam turbine to produce electricity, and then condensed back to a liquid state. This condensing step is achieved using a water source to reject the heat not extracted by the turbine.

2.4 Fuel Cost Calculations

The last metric evaluated for the various reactor designs was the front-end fuel cycle cost. The fuel cycle cost considers the cost of fuel procurement from the mining to the complete fabricated fuel. This value is calculated by applying a multiplier constant at each stage of the process to the mass of material that undergoes the process. These processes include the mining and milling of natural uranium, the conversion of natural uranium, the enrichment of the uranium, the disposal of the depleted uranium, and the cost of fabricating the fuel. The multiplier constants are shown in Table 2.7. From Table 2.7, the fuel fabrication cost dominates the cost metric due to being two orders of magnitude greater than all other multiplier constants. The high fabrication cost is due to uranium nitride TRISO fuel being a newer fuel form and not benefiting from an established supply chain. Table 2.8 shows the multiplier constants used for the LWR cost calculations done for an LWR and SMR to compare to the HTGR reactors.

Table 2.6: Multiplier constants for water use calculations [33]

Process	Multiplier	Units
Mining/Milling	$8.5E-01$	$ML/MTNU$
Conversion	$6.5E-02$	$ML/MTNU$
Enrichment	$2.9E-05$	ML/SWU
Deconversion	$5.3E-04$	$ML/MTDU$
Fabrication	$1.41E-01$	$ML/MTIHM$
Reactor Operation	$2.37E04$	$ML/GWe-y$
Waste conditioning	$4.83E-01$	$ML/MTIHM$
Land Burial	$2.3E-04$	$ML/MTDU$
Repository	$1.43E-01$	$km^2/MTIHM$

Table 2.7: Costs associated with TRISO fuel fabrications [38]

Category	Cost	Multiplier Parameter
Mining/milling	110,000 $\frac{USD}{MTNU}$	$M_{natural}(\frac{MTNU}{GWe-year})$
Conversion	12,000 $\frac{USD}{MTNU}$)	$M_{natural}(\frac{MTNU}{GWe-year})$
Enrichment	100 $\frac{USD}{SWU}$	$SWU(\frac{SWU}{GWe-year})$
Depleted Uranium Disposal	4,000 $\frac{USD}{MTDU}$	$M_{DU}(\frac{MTDU}{GWe-year})$
Fuel fabrication	10,000,000 $\frac{USD}{MTIHM}$)	$M_{flow}(\frac{MTIHM}{GWe-year})$

Table 2.8: Costs associated with LWR fuel fabrications [33]

Category	Cost	Multiplier Parameter
Mining/milling	135,000 $\frac{USD}{MTNU}$	$M_{natural}(\frac{MTNU}{GWe-year})$
Conversion	12,000 $\frac{USD}{MTNU}$	$M_{natural}(\frac{MTNU}{GWe-year})$
Deconversion	6,000 $\frac{USD}{MTDU}$	$M_{DU}(\frac{MTDU}{GWe-year})$
Enrichment	97 $\frac{USD}{SWU}$	$SWU(\frac{SWU}{GWe-year})$
Depleted Uranium Disposal	587,000 $\frac{USD}{MTDU}$	$M_{DU}(\frac{MTDU}{GWe-year})$
Fuel fabrication	350,000 $\frac{USD}{MTIHM}$	$M_{flow}(\frac{MTIHM}{GWe-year})$

2.5 Activity Calculations

Equation 2.8 is used to calculate the activity of the SNF&HLW for a given time after reactor operations. The activity of the SNF&HLW, A(t), is calculated using Serpent at 100 and 100,000 years after reactor shutdown. The initial fissile mass, $M_{fissile}$, and total fuel mass M_{flow} are then used to energy normalize the activity. The activity is evaluated at 100 and 100,000 years to compare the fuel's disposal hazard after the initial cooling period, 100 years, and the long-term potential exposure if the waste was released at 100,000 years [33].

$$Activity(t) * M_f/M_{fission} \tag{2.8}$$

Chapter 3

Results

3.1 Design optimization

Material optimization sweeps were performed to find the best possible geometric configuration for the micro-reactor for each moderator. Due to all of the metrics of interest being dependent on the discharge burnup of the nuclear reactor fuel, the optimization was done based on maximizing the discharge burnup. The outer dimensions of the reactor were held constant, and the fuel blocks' TRISO packing fraction and lattice pitch varied. Changing the TRISO packing fraction increases or decreases the total fuel volume in the reactor and, therefore, the fuel-to-moderator ratio within the reactor. Changing the lattice pitch varies how spread out the fuel elements are within the reactor, changing the distance between them and the ratio of the moderator to reflector within the reactor. The TRISO packing fraction was varied from 5 to 50 percent, and the lattice pitch from 2.0 to 2.5cm for all five moderator material designs.

Figure 3.1 shows a contour plot of the optimization sweep performed for the reference graphite moderated prismatic mHTGR. The X-axis shows the changing lattice pitch

from 2.0 to 2.5cm. The lattice pitch references the spacing between the fuel and coolant channels in the prismatic blocks within the reactor. The fuel elements will be placed further apart in the reactor for a larger lattice pitch. The number of lattices, their size, and the number of fuel and coolant channels in each block remain constant. Therefore, changes in lattice pitch do not change the mass of fuel within the reactor. Since the number of fuel blocks is not changed, a smaller lattice pitch leads to a smaller core and, therefore, a larger reflector since the outer reactor diameter is constant.

The Y-axis shows the variation in the TRISO packing fraction within the fuel elements in the reactor. The packing fraction is the percentage of the fuel compact volume comprised of TRISO fuel particles. In this way, a larger TRISO packing fraction means more fuel is in the reactor system. Since the additional fuel is added by packing more fuel into the existing fuel elements. Changing the fuel volume changes the fuel-to-moderator ratio within the reactor.

The contour plot's color shows the fuel's discharge burnup within the reactors in GWd per ton. The scale runs from dark blue at 0 to bright red at greater than 90GWd/ton. The black lines on the contour plot are lines of constant discharge burnup. The purpose of this plot is to locate the optimal configuration for the graphite mHTGR. The primary goal is to reduce the mass of spent nuclear fuel and high-level waste, the volume of low-level nuclear waste produced, and the mass of depleted uranium produced per unit of energy generated. The secondary goal is to reduce the cost of the initial fuel loaded into the reactor per unit of energy that will be generated. Thirdly, the goal is to limit the environmental impact of the reactor operation. The environmental impact of the reactor operation is evaluated based on the mass of carbon dioxide released, the volume of water consumed, and the mass of natural uranium utilized per unit of energy generated. The last metrics study is the activity of nuclear waste 100 and 100,000 years after reactor shutdown per unit of

energy generated. Here, the objective is to avoid significant increases in nuclear waste activity compared to traditional reactor technologies on a per-unit energy basis. All of these metrics are driven by the discharge burnup of the nuclear fuel and are reduced with increasing discharge burnup. Therefore, according to all the desired metrics, the optimal design will be the design with the highest burnup.

Looking at Figure 3.1, it can be seen that as a general trend, the discharge burnup increases with increasing lattice pitch. An exception to this trend occurs at a ten percent TRISO packing fraction. When the TRISO packing fraction is at or near ten percent, the discharge burnup increases with increasing lattice pitch up to a lattice pitch of 2.4cm, and beyond a lattice pitch of 2.4cm, the discharge burnup begins to decrease with increasing lattice pitch. The increasing discharge burnup with increasing lattice pitch indicates that with more space between the fuel elements, neutrons are more likely to be born in one fuel element and reach thermal energies after traveling to another fuel element, causing an additional fission in the new fuel element. The trade-off with increased distance between fuel elements is that this increases the reactor core size and places the outer fuel elements closer to the edge of the reactor. Having fuel closer to the reactor edge increases the chances that neutrons will leak out of the reactor rather than being slowed to thermal energies in the reactor and causing additional fissions.

Looking at the trend between the TRISO packing fraction and discharge burnup in the graphite system optimized in Figure 3.1, it is seen that increasing the TRISO packing fraction generally causes a decrease in the discharge burnup. This trend of decreased discharge burnup with increasing TRISO packing fraction is seen only in TRISO packing fractions above 10 percent. The discharge burnup increases with increasing TRISO packing fraction up to the inflection point at 10 percent TRISO packing.

This inflection point represents the optimal fuel-to-moderator ratio. The fuel-to-moderator ratio represents the reactor system's fuel volume versus the moderator material's volume. With too much fuel, the system is considered under-moderated. In under-moderated systems, moderator material is insufficient to slow the neutrons born from fission events to thermal energies before leaking. The high leakage system leads to lower discharge burnup since fewer neutrons are in the system to maintain the chain fission reaction. With fewer neutrons, the system will become sub-critical with more fuel not being burned, reducing the discharge burnup. Above the ten percent TRISO packing fraction, the discharge burnup decreases with increasing fuel due to the under-moderated system. For the values below the ten percent TRISO packing fraction, the system becomes over-moderated. In this case, the neutrons are slowed down too quickly and are parasitically absorbed by the moderator material before they have a chance to cause additional fission reactions. In the under-moderated systems, increasing the lattice pitch increases discharge burnup by moving more of the fuel toward the edge of the reactor, where the neutrons are more likely to be at thermal energies after traveling from the center of the reactor.

Overall, Figure 3.1 shows the optimization sweeps performed to find the optimal configuration of a graphite mHTGR based on finding the highest possible discharge burnup. From Figure 3.1, the optimal configuration for a graphite mHTGR is a ten percent TRISO packing fraction in the fuel elements with a 2.4cm lattice pitch in the prismatic fuel blocks. This optimized graphite design will be used as the benchmark with which the composite moderator designs are compared.

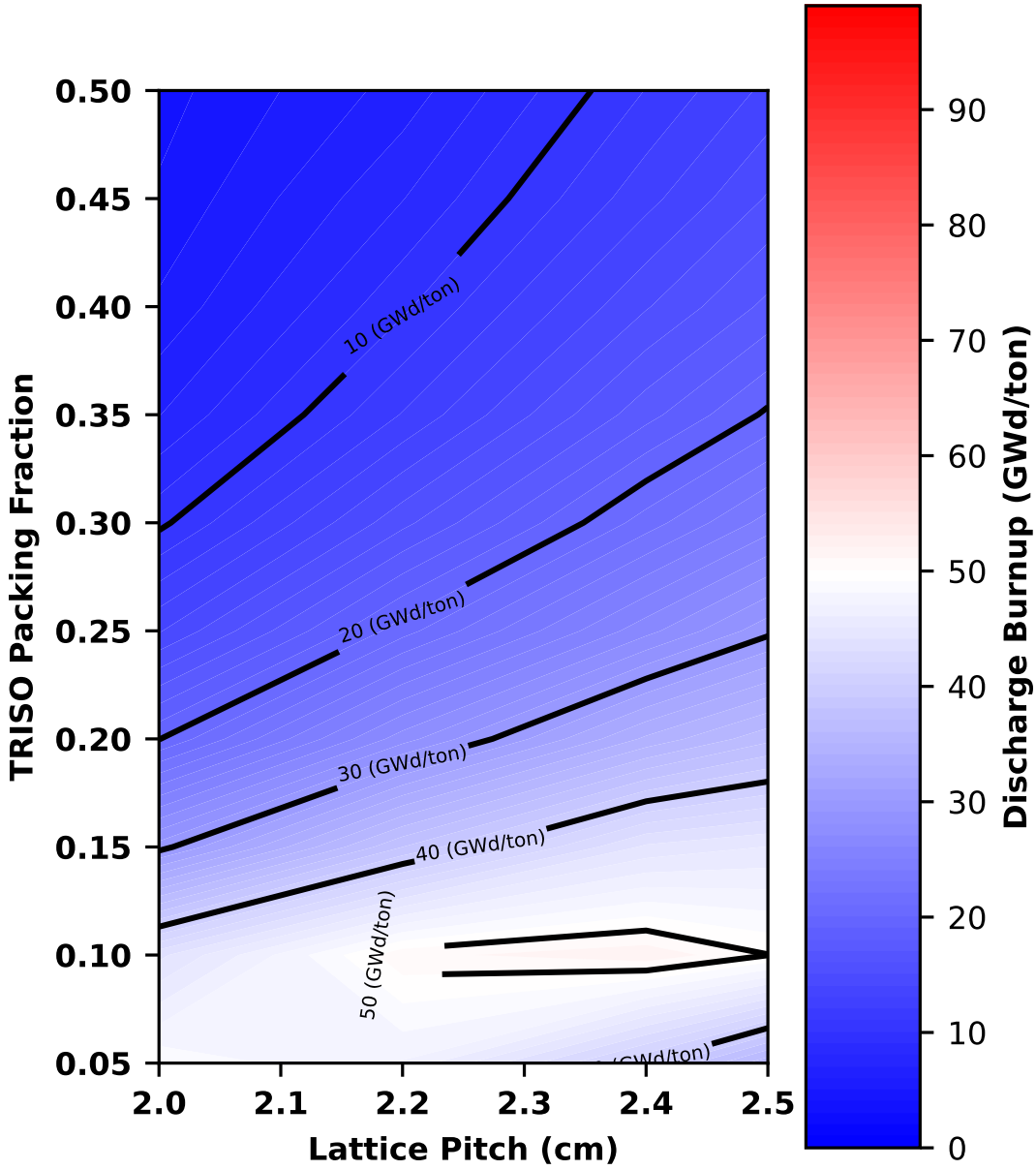

Figure 3.1: Contour plot of discharge burnup as a function of lattice pitch and TRISO packing fraction for the reference graphite design

Figure 3.2 shows a contour plot of the optimization sweep performed for the $MgOBeO$ moderated prismatic mHTGR. From Figure 3.2, it can be seen that the effect of the lattice pitch on the discharge burnup is different depending on whether the TRISO packing faction is above or below 10 percent. When the TRISO packing fraction is above ten percent, the lattice pitch increases the discharge burnup for a constant TRISO packing fraction. This increase in burnup with increased lattice pitch indicates that a larger reactor core with a smaller reflector region is more optimal at higher TRISO packing fractions. The benefit of a larger core size points to a benefit in the fuel elements being placed further apart, allowing more space for neutrons to reach thermal energies when being born in one fuel element and then traveling to another. In the region below the ten percent TRISO packing fraction, the lattice pitch reduces discharge burnup. At a low TRISO packing fraction, around 8 percent, a local maximum discharge burnup is seen at a lattice pitch of 2.2cm. This maximum represents the point that best balances the separation of fuel elements to allow neutrons to reach thermal energies as they travel between fuel elements and the benefits of a larger reflector region in reducing neutron leakage by scattering neutrons back into the reactor core.

Looking at the TRISO packing fraction shown along the Y-axis, it can be seen that for a set lattice pitch, the discharge burnup increases with increasing TRISO packing fraction to a local maximum at 10 percent TRISO packing and then decreases with further increasing TRISO packing fraction. Varying the TRISO packing fraction varies the fuel-to-moderator ratio by increasing the fuel volume for the same moderator volume. For the prismatic design, the MgO matrix that contains the TRISO particles is not considered a moderator. Therefore, the increase in TRISO packing fraction does not reduce the moderator material by its addition. This effect on the fuel-to-moderator ratio leads to the conclusion that the designs with less than

a 10 percent TRISO packing are over-moderated. The systems with over a 10 percent TRISO packing fraction are under-moderated.

As the TRISO packing fraction increases, the fuel-to-moderator ratio is increased. Increasing the fuel-to-moderator ratio increases thermal utilization and decreased residence escape probability, as well as fast and thermal non-leakage factors. The increased thermal utilization factor is driven by the increase in fuel volume, making it more likely for a thermal neutron in the reactor to be absorbed in the fuel rather than another material. The increase in the residence escape probability comes from the reduction in moderator volume relative to the fuel. The neutrons, therefore, take more time and travel further as they slow to thermal energies and have more opportunities to be absorbed during the slowing down process. The reduced moderator also drives the fast and thermal non-leakage probabilities compared to fuel; with less moderator material, the neutrons are more likely to leak out of the system before interacting. Based on these values, a higher fuel-to-moderator ratio is favorable for the thermal utilization factor. In contrast, a low fuel-to-moderator ratio favors higher residence escape probability and non-leakage factors. Therefore, the TRISO packing fraction variation seeks the optimum where the opposing benefits are best balanced.

From Figure 3.2, the optimization sweeps that were performed to find the optimal configuration of a $MgOBeO$ moderated mHTGR based on finding the highest possible discharge burnup are shown. From Figure 3.2, the optimal configuration for a $MgOBeO$ moderated mHTGR is found to be a ten percent TRISO packing fraction in the fuel elements with a 2.4cm lattice pitch in the prismatic fuel blocks. This optimized $MgOBeO$ moderated design will be used to calculate all the evaluated metrics.

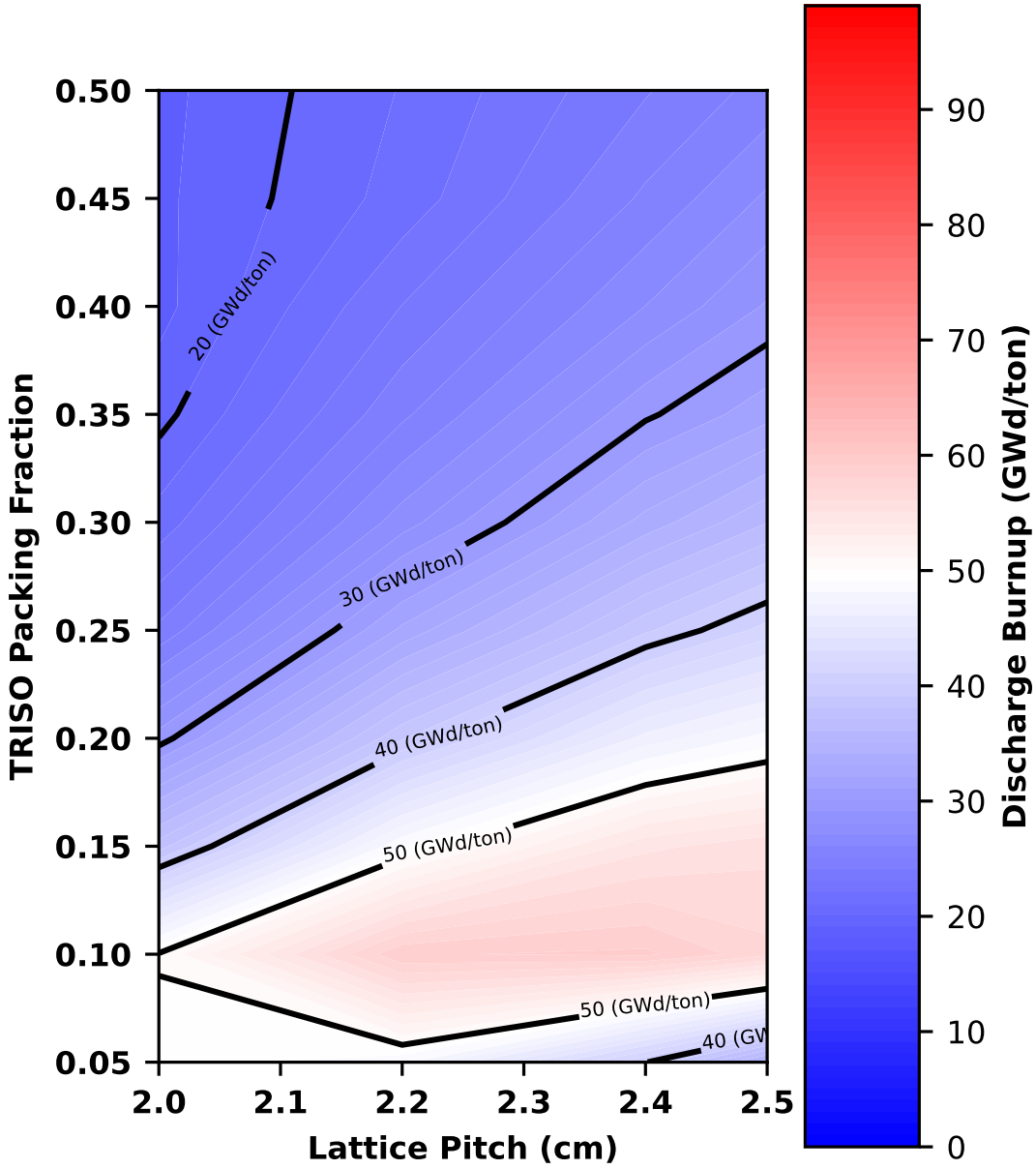

Figure 3.2: Contour plot of discharge burnup as a function of lattice pitch and TRISO packing fraction for the MgO-BeO concept

Figure 3.3 shows a contour plot of the optimization sweep performed for the $MgOBe$ moderated prismatic mHTGR. From Figure 3.3, it can be seen that the effect of the lattice pitch on the discharge burnup is different depending on whether the TRISO packing faction is above or below fifteen percent. When the TRISO packing fraction is above fifteen percent, the lattice pitch increases the discharge burnup for a constant TRISO packing fraction. This increase in burnup with increased lattice pitch indicates that a larger reactor core with a smaller reflector region is more optimal at higher TRISO packing fractions. The benefit of a larger core size points to a benefit in the fuel elements being placed further apart, allowing more space for neutrons to reach thermal energies when being born in one fuel element and then traveling to another. In the region below fifteen percent of the TRISO packing fraction, the same general trend of increased discharge burnup with increased lattice pitch is observed. This trend of increased discharge burnup with increased lattice pitch does not hold for TRISO packing fractions from around seven to thirteen percent and a lattice pitch over about 2.45cm. This indicated that ,the larger core with a larger lattice pitch leads to increased leakage, which is greater than increased thermal utilization in this region.

Looking at the TRISO packing fraction shown along the Y-axis, it can be seen that for a set lattice pitch, the discharge burnup increases with increasing TRISO packing fraction to a local maximum at 10 percent TRISO packing and then decreases with further increasing TRISO packing fraction. Varying the TRISO packing fraction varies the fuel-to-moderator ratio by increasing the fuel volume for the same moderator volume. For the prismatic design, the MgO matrix that contains the TRISO particles is not considered a moderator. Therefore, the increase in TRISO packing fraction does not reduce the moderator material by its addition. This effect on the fuel-to-moderator ratio leads to the conclusion that the designs with less than

a 10 percent TRISO packing are over-moderated. The systems with over a 10 percent TRISO packing fraction are under-moderated.

As the TRISO packing fraction increases, the fuel-to-moderator ratio is increased. Increasing the fuel-to-moderator ratio increases thermal utilization and decreased residence escape probability, as well as fast and thermal non-leakage factors. The increased thermal utilization factor is driven by the increase in fuel volume, making it more likely for a thermal neutron in the reactor to be absorbed in the fuel rather than another material. The increase in the residence escape probability comes from the reduction in moderator volume relative to the fuel. The neutrons, therefore, take more time and travel further as they slow to thermal energies and have more opportunities to be absorbed during the slowing down process. The reduced moderator also drives the fast and thermal non-leakage probabilities compared to fuel; with less moderator material, the neutrons are more likely to leak out of the system before interacting. Based on these values, a higher fuel-to-moderator ratio is favorable for the thermal utilization factor. In contrast, a low fuel-to-moderator ratio favors higher residence escape probability and non-leakage factors. Therefore, the TRISO packing fraction variation seeks the optimum where the opposing benefits are best balanced.

From Figure 3.3, the optimization sweeps that were performed to find the optimal configuration of a $MgOBe$ moderated mHTGR based on finding the highest possible discharge burnup are shown. From Figure 3.3, the optimal configuration for a $MgOBe$ moderated mHTGR is found to be a ten percent TRISO packing fraction in the fuel elements with a 2.2cm lattice pitch in the prismatic fuel blocks. This optimized $MgOBe$ moderated design will calculate all the evaluated metrics.

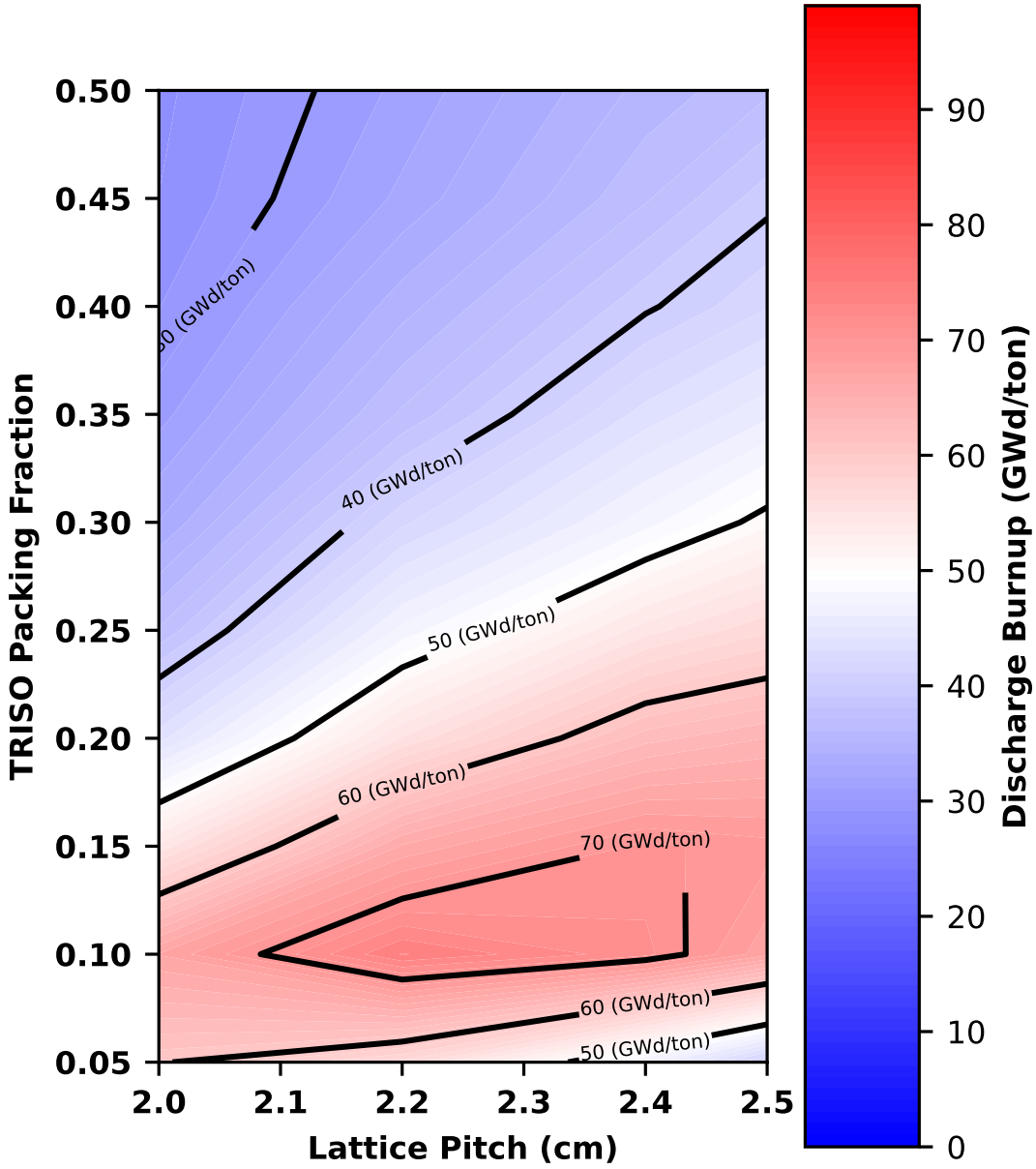

Figure 3.3: Contour plot of discharge burnup as a function of lattice pitch and TRISO packing fraction for the MgO-Be design

Figure 3.4 shows a contour plot of the optimization sweep performed for the $MgOYH_{x=1.9}$ moderated prismatic mHTGR. From Figure 3.4 it can be seen that increasing the lattice pitch leads to an increase in the discharge burnup for a constant TRISO packing fraction. The larger lattice pitches create larger core regions with reactors of constant size, reducing the reflector thickness. The increase in discharge burnup with increased lattice pitch indicated that with the fuel elements further separated, the neutrons burned in one fuel element are more likely to reach thermal energies and be absorbed by the time they reach another. This trend of increasing discharge burnup with increasing lattice pitch is only broken for TRISO packing fractions above thirty-five percent and only for lattice pitches beyond 2.4cm.

For the TRISO packing fraction, it can be seen that an increase in the TRISO packing fraction leads to an increase in the discharge burnup of the reactor design. As the TRISO packing fraction increases, the fuel-to-moderator ratio is increased. Increasing the fuel-to-moderator ratio increases thermal utilization and decreased residence escape probability, as well as fast and thermal non-leakage factors. The increased thermal utilization factor is driven by the increase in fuel volume, making it more likely for a thermal neutron in the reactor to be absorbed in the fuel rather than another material. The increase in the residence escape probability comes from the reduction in moderator volume relative to the fuel. The neutrons, therefore, take more time and travel further as they slow to thermal energies and have more opportunities to be absorbed during the slowing down process. The reduced moderator also drives the fast and thermal non-leakage probabilities compared to fuel; with less moderator material, the neutrons are more likely to leak out of the system before interacting. Based on these values, a higher fuel-to-moderator ratio is favorable for the thermal utilization factor. In contrast, a low fuel-to-moderator ratio favors higher residence escape probability and non-leakage factors. Therefore, the TRISO packing fraction

variation seeks the optimum where the opposing benefits are best balanced. The TRISO packing fraction and the discharge burnup increase together, meaning that the thermal utilization factor is the limiting factor for further increases in reactivity and, therefore, discharge burnup. The thermal utilization factor has a greater effect than the combined effect of the non-leakage factors and the residence escape probability for two main reasons. Firstly, a large amount of hydrogen within the yttrium hydride is an excellent moderator. It slows down the fast neutrons born from fission before reducing the time and distance they have to be absorbed or leak. The second reason is that the yttrium within yttrium hydride has a high absorption cross section for thermal neutrons and, therefore, parasitically absorbs thermal neutrons, reducing the thermal utilization factor. Adding more fuel through increased TRISO packing fraction counters the reduction in the thermal utilization factor caused by the yttrium. From Figure 3.4, the optimization sweeps that were performed to find the optimal configuration of a $Pris_{Y}H_{x=1.9}$ moderated mHTGR based on finding the highest possible discharge burnup are shown. From Figure 3.4, the optimal configuration for a $Pris_{Y}H_{x=1.9}$ moderated mHTGR is found to be forty-five percent TRISO packing fraction in the fuel elements with a 2.4cm lattice pitch in the prismatic fuel blocks. This optimized $Pris_{Y}H_{x=1.9}$ moderated design will be used to calculate all the evaluated metrics.

Figure 3.5 shows a contour plot of the optimization sweep performed for the $MgOZrH_{x=1.6}$ moderated prismatic mHTGR. Looking at the lattice pitch changes along the X-axis in Figure 3.5 for a set TRISO packing fraction, the trend can be seen that below a packing fraction of twenty percent, the discharge burnup increases with increasing lattice pitch. The larger lattice pitches create larger core regions with reactors of constant size, reducing the reflector thickness.

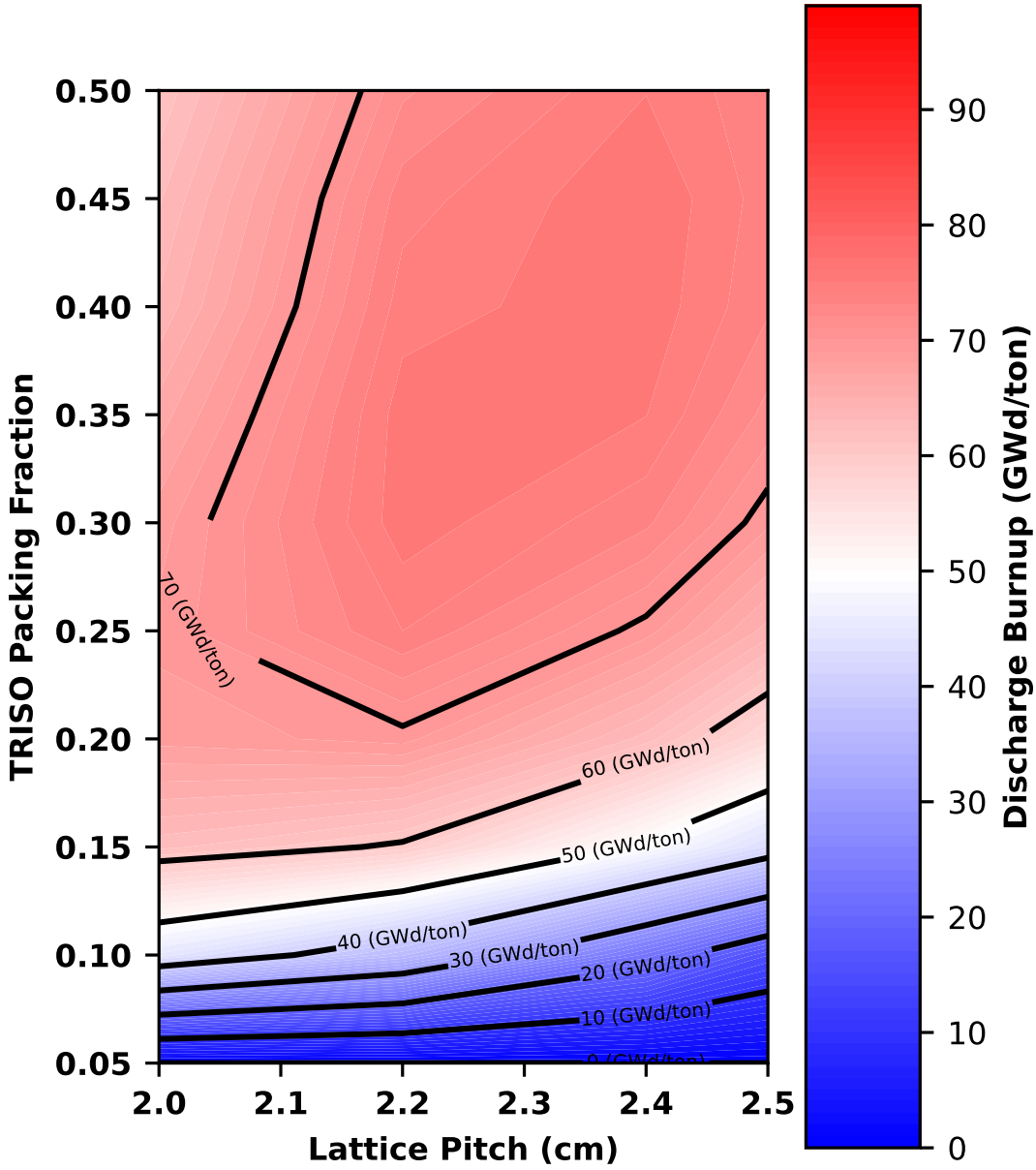

Figure 3.4: Contour plot of discharge burnup as a function of lattice pitch and TRISO packing fraction for the $MgO - YH_{x=1.9}$ concept.

The increase in discharge burnup with increased lattice pitch indicated that with the fuel elements further separated, the neutrons burned in one fuel element are more likely to reach thermal energies and be absorbed by the time they reach another. This trend of increasing discharge burnup for increasing lattice pitch breaks down past a TRISO packing of twenty percent. For TRISO packing fractions higher than twenty percent, the highest discharge burnup is seen for packing fractions in the middle of the range studied. This shift from the highest lattice pitches is due to higher leakage and increased fuel-to-moderator ratio at the higher TRISO packing fractions. The large lattice pitch worsens the increased leakage by moving fuel elements closer to the edge of the reflector.

Looking at the Y-axis in Figure 3.5, it is seen that the discharge burnup increases with increasing TRISO packing fraction up to a TRISO packing fraction of forty percent. As the TRISO packing fraction increases, the fuel-to-moderator ratio is increased. Increasing the fuel-to-moderator ratio creates an increased thermal utilization factor, decreased residence escape probability, and fast and thermal non-leakage factors. The increased thermal utilization factor is driven by the increase in fuel volume, making it more likely for a thermal neutron in the reactor to be absorbed in the fuel rather than another material. The increase in the residence escape probability comes from the reduction in moderator volume relative to the fuel. The neutrons, therefore, take more time and travel further as they slow to thermal energies and have more opportunities to be absorbed during the slowing down process. The reduced moderator also drives the fast and thermal non-leakage probabilities compared to fuel; with less moderator material, the neutrons are more likely to leak out of the system before interacting. Based on these values, a higher fuel-to-moderator ratio is favorable for the thermal utilization factor. In contrast, a low fuel-to-moderator ratio favors higher residence escape probability and non-leakage factors. Therefore, the TRISO packing fraction

variation seeks the optimum where the opposing benefits are best balanced. This balance is found at a thirty percent TRISO packing fraction.

From Figure 3.5, the optimization sweeps that were performed to find the optimal configuration of a $Pris_ZrH_{x=1.6}$ moderated mHTGR based on finding the highest possible discharge burnup are shown. From Figure 3.5, the optimal configuration for a $Pris_ZrH_{x=1.6}$ moderated mHTGR is found to be thirty percent TRISO packing fraction in the fuel elements with a 2.2cm lattice pitch in the prismatic fuel blocks. This optimized $Pris_ZrH_{x=1.6}$ moderated design will be used to calculate all the evaluated metrics.

Table 3.1 shows the optimum configurations for each moderator material regarding the TRISO packing fraction and lattice pitch. The graphite and the beryllium cases have the same optimum configuration with 10 percent TRISO packing and a lattice pitch of 2.4cm. The beryllium oxide is optimized for the same packing fraction but with a smaller lattice pitch of only 2.2cm compared to the beryllium and graphite cases. The reduced lattice pitch puts the fuel closer together, providing more reflector around the fueled region and reducing leakage to account for the reduced moderation of the beryllium oxide compared to the beryllium case due to the addition of oxygen. The yttrium hydride cases have an optimal lattice pitch of 2.4cm, as was seen in the beryllium and graphite, but with a greatly increased packing fraction of 45 percent. The higher packing fraction is optimal in the yttrium cases because the hydrogen in the yttrium hydride is a better moderator than the graphite or beryllium. Additionally, a higher fuel volume is needed to overcome the parasitic absorption of the yttrium, reducing the thermal utilization factor. For the zirconium hydride, the optimal packing fraction is 30 percent, while the optimal lattice pitch is 2.2cm.

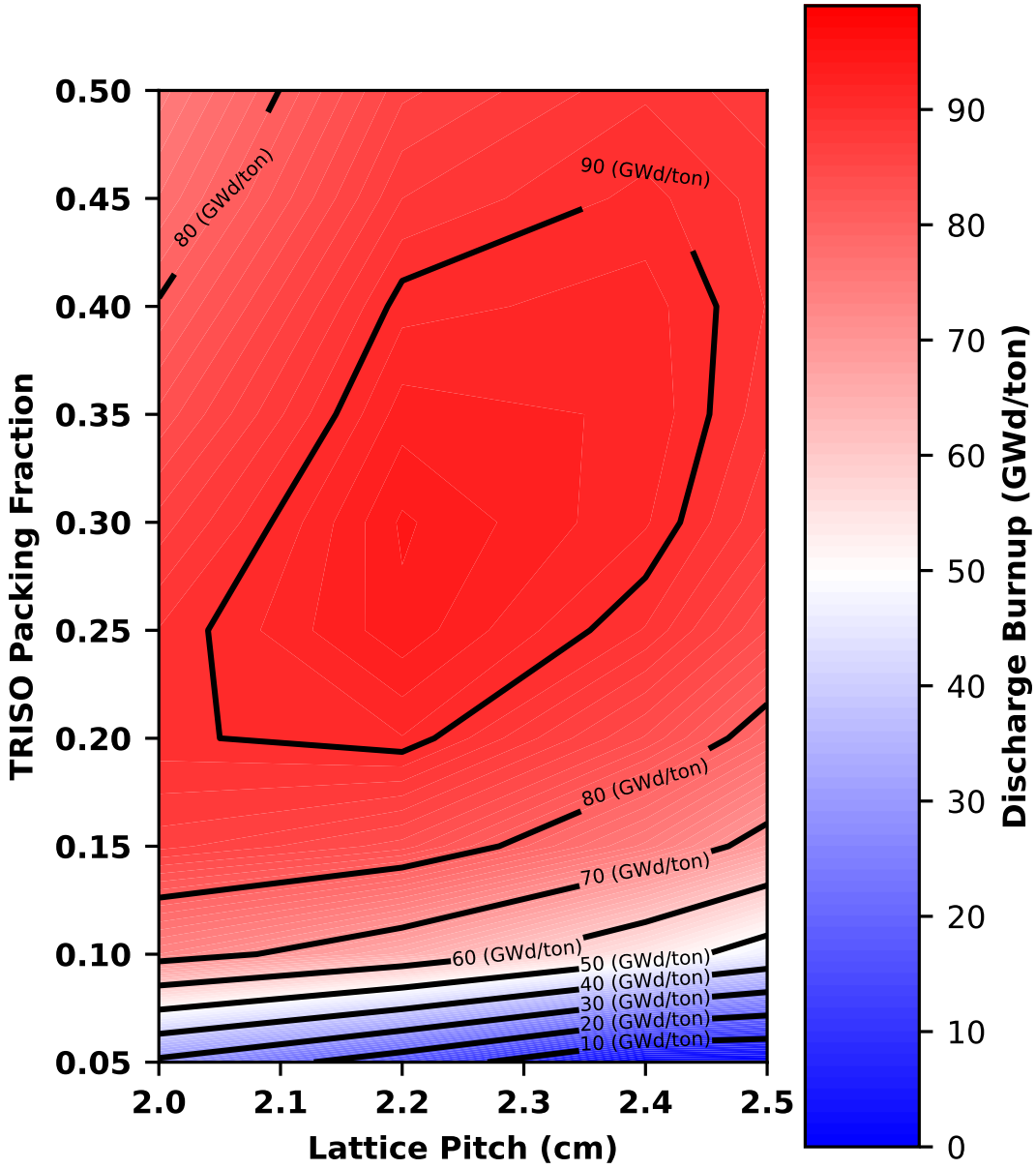

Figure 3.5: Contour plot of discharge burnup as a function of lattice pitch and TRISO packing fraction for the $MgO - ZrH_{x=1.6}$ concept.

Table 3.1: Optimal prismatic core configuration for discharge burnup.

Moderator Material	TRISO packing fraction %	Fuel pin lattice pitch (cm)
Graphite	10	2.4
$MgOBeO$	10	2.4
$MgOBe$	10	2.2
$MgOYH_{x=1.9}$	45	2.4
$MgOZrH_{x=1.6}$	30	2.2

The reduced TRISO packing fraction compared to the yttrium is due to the zirconium being less likely to parasitically absorb thermal neutrons, requiring less fuel. The zirconium hayride has better moderation over the graphite and beryllium cases and can support a higher TRISO packing fraction.

3.2 Waste Metric

The first set of metrics evaluated to determine the benefits of using composite moderators in mHTGRs is the nuclear waste metrics. For the nuclear waste metrics, the mass of spent nuclear fuel and high-level waste (SNF&HLW), the mass of depleted uranium (DU), and the volume of low-level waste (LLW) were all evaluated on a per unit energy generated basis.

Figure 3.6 shows the results for the SNF&HLW calculations. Here, the SNF&HLW is calculated for each reactor design on a per unit of energy generated annually basis. The normalization based on the energy generated allows for a one-to-one comparison with other reactor concepts on different scales. In this case, the composite moderator mHTGR results are compared with a graphite mHTGR at the same size, considered the current state of the art, and labeled as the reference case. The percentage reduction in energy normalized mass of SNF&HLW for each moderator concept compared to the reference graphite design is displayed in Figure 3.6 above the bar of each composite moderator result. Additionally, the composite moderator results are compared to a light water small modular reactor from the literature shown in gray and labeled SMR [12]. The results from a large light water reactor from the literature are also shown in the plot in black and labeled as LWR [12].

Looking at Figure 3.6, it is clear that mHTGRs produce less mass of SNF&HLW per

unit of energy generated compared to large LWRs and light water SMRs. A large reduction can already be seen when comparing only the graphite reference to the LWR and SMR. Additional reductions are observed in the composite moderator mHTGRs. Compared to the graphite reference, the beryllium oxide reactor produces 12.6 percent less mass of SNF&HLW per unit of energy generated. The beryllium case shows a 302 percent reduction in mass of SNF&HLW per unit of energy generated, and the yttrium hydride slightly greater reduction of 31.8 percent mass of SNF&HLW per unit of energy generated. The best performer is the zirconium hydride, showing a 45.0 percent reduction in mass of SNF&HLW per unit of energy generated compared to the graphite reference reactor. With the graphite reference already performing better when compared with traditional light water reactor technologies, all the composite moderators show good improvement.

The decrease in mass of SNF&HLW per unit of energy generated in the graphite HTGR compared to the light water designs is due to the mHTGR using fuel with a higher enrichment of uranium 235. Traditional light water reactors such as the LWR and SMW are considered here to use fuel with less than 5 percent uranium 235. In contrast, all mHTGR designs use fuel enriched to 19.5 percent uranium 235. The higher enrichment in the mHTGRs allows for greater discharge burnup. The reactor can maintain criticality after more fuel has been burned due to the increased uranium 235 atoms available to cause fissions. This higher fuel enrichment allows the mHTGRs to achieve higher burnups despite having greater neutron leakage than large light water reactors due to their smaller size. The additional neutron leakage seen in smaller reactor systems is the primary cause of the SMR producing more mass of SNF&HLW per unit of energy generated compared to the LWR. The SMR and LWR are light water reactors using less than 5 percent enriched uranium 235 fuel. However, the smaller dimensions of SMR lead to increased neutron leakage. The increase in

neutron leakage means fewer neutrons are available to cause fissions; therefore, more fuel is required to maintain criticality. With more fuel required, the reactor becomes sub-critical earlier in its lifetime as fuel is burned and the number of uranium 235 atoms decreases.

The composite moderator mHTGRs achieve a lower mass of SNF&HLW per unit of energy generated than the graphite reference case by reaching a higher discharge burnup. The composite moderators have higher moderating power when compared to graphite, allowing for reduced leakage from the system and, therefore, an increase in discharge burnup. In the cases of the hydride moderators, the high moderating power of the composite moderators allows for more fuel in the reactor and, therefore, a higher discharge burnup with the increase in uranium 235 atoms within the system. In addition to the increase in TRISO packing in the hydride cases, all the composite moderators use uranium nitrite (UN) TRISO particles. In contrast, the graphite reference uses uranium oxy-carbide (UCO) TRISO. The UN and UCO TRISO's were set to be the same size. However, the UN has a higher uranium atom fraction than UCO; therefore, one UN TRISO has more uranium atoms than a UCO TRISO. The increased fuel in the composite moderator helps take advantage of the higher moderator power of the composite moderators and achieve higher discharge burnup. The increased discharge burnup produced by the composite moderator designs leads to a reduction in the mass of SNF&HLW per unit of energy generated when compared to LWR, light water SMR, and a graphite reference mHTGR. This reduction makes the composite moderators an attractive design for micro-reactors.

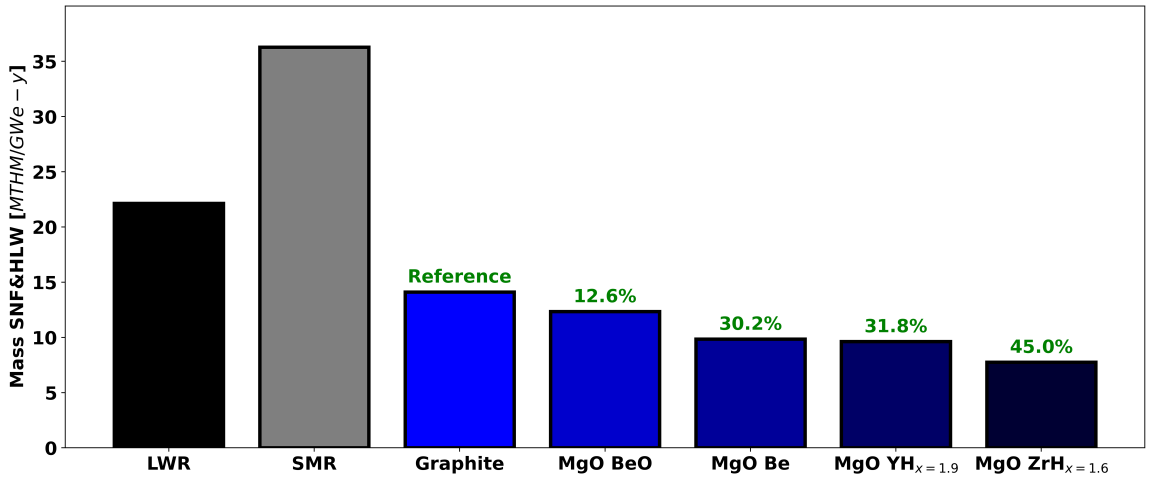

Figure 3.6: Energy normalized mass of SNF&HLW for large-scale LWR, SMR, graphite micro-prismatic reference and prismatic IMF fuel concepts

The next metric for the nuclear waste to be evaluated is the energy-normalized volume of low-level waste seen in Figure 3.7. The first 2 bars, the black, LWR, and gray, SMR, show the same large light water reactor and small module light water reactor from literature previously shown [12]. The graphite bar labeled reference shows the optimized graphite moderated mHTGR. The energy-normalized volume of low-level waste in the graphite reference is higher than in the LWR and SMR cases. The higher values in the graphite reference case are due to the prismatic graphite blocks in the reactor's core being considered low-level waste and, therefore, being included in the calculations. One of the main motivations for using magnesium oxide as the host matrix in composite moderator cases is its irradiation stability. For this reason, the moderator blocks from the composite moderator designs are not considered in the volume of low-level waste calculations for irradiation stability. Looking at the composite moderator values of the volume of low-level waste per unit of energy generated, all four concepts show reductions compared to the graphite reference case. The beryllium oxide case shows a 31.4 percent reduction in the volume of low-level waste per unit of energy generated. The beryllium case shows a higher 37.9 percent reduction in the volume of low-level waste per unit of energy generated driven by the higher discharge burnup achieved with the better-moderating power of the beryllium with the oxygen removed. The yttrium case again shows a slight improvement over the beryllium case as the higher moderation of the hydrogen produces a higher discharge burnup, overcoming the parasitic absorption of the yttrium. This increase produces a 38.5 percent reduction in the volume of low-level waste per unit of energy generated compared to the graphite reference case. Again, the zirconium hydride performs the best with the highest discharge burnup, producing a 43.5 percent reduction in the volume of low-level waste per unit of energy generated compared to the graphite reference case.

Comparing the composite moderator cases to the LWR and SMR cases, it is seen that all four composite moderators are close to the values of the SMR and LWR, with all but the beryllium oxide value falling between that of the LWR and SMR. This result of the mHTGRs being in the same order as the LWR and SMR is good, as it would be expected for smaller reactor systems to underperform larger reactor systems due to higher leakage, leading to lower discharge burnups. The composite mHTGRs overcome this challenge in two main ways: the higher moderating power of the composite moderators leads to higher discharge burnups. Second, the higher outlet temperatures of the coolant in HTGRs allow for better thermal efficiency in converting thermal power to electrical power than in light-water reactor systems. Additionally, the use of the irradiation stable magnesium oxide in the composite moderators shows a significant advantage over the current state-of-the-art mHTGR using graphite due to higher discharge burnup and especially due to not having to account for the matrix moderator block as low-level waste due to the higher irradiation stability compared to graphite.

Figure 3.8 shows each reactor concept's energy-normalized mass of depleted uranium. The black bar, LWR, is for a large light water reactor from literature, and the gray bar, SMR, is for a small module light water reactor also from literature [12]. The SMR produces more energy-normalized depleted uranium compared to the LWR due to the LWR achieving higher discharge burnups. The higher discharge burnups seen in the LWR are driven by the larger geometry of the LWR, leading to fewer neutrons leaking and, therefore, less fuel mass required to maintain criticality.

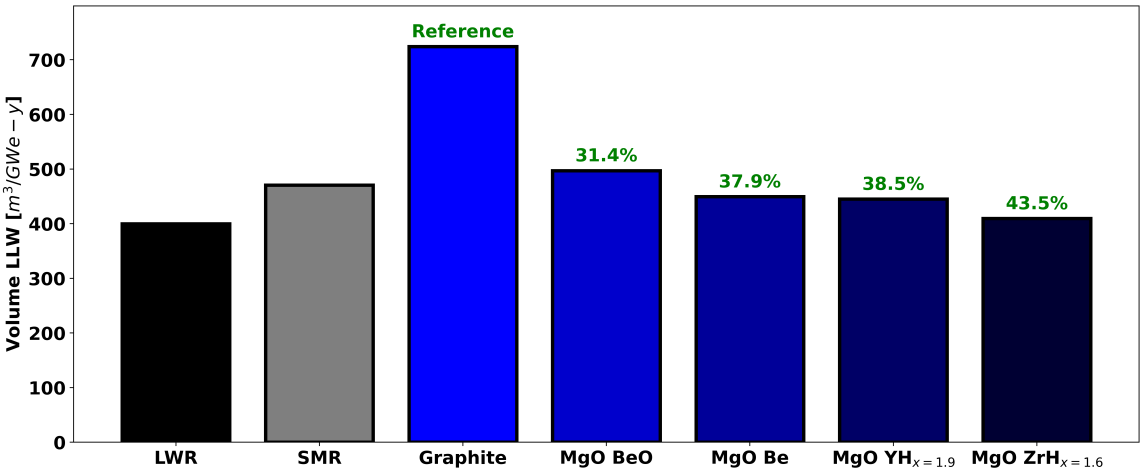

Figure 3.7: Energy normalized volume of low level waste for large-scale LWR, SMR, graphite micro-prismatic reference and prismatic IMF fuel concepts

Since less fuel mass is needed to maintain criticality, the reactor can burn for longer; as the fuel is depleted, the mass of available uranium 235 is decreased, and the LWR needs less uranium 235 to maintain criticality and, therefore, remains critical with more fuel being burned up. The graphite bar labeled as reference is the optimized graphite mHTGR. The graphite mHTGR shows significantly increased production of depleted uranium per unit of energy generated annually. The higher fuel enrichment in the mHTGRs drives this increase in energy normalized depleted uranium The enrichment process considers the enrichment level of natural uranium, depleted uranium, the nuclear fuel, and the mass of each being used. The enrichment of both natural and depleted uranium is a constant. Therefore, the only change in enrichment is the fuel being produced. A higher fuel enrichment requires more uranium 235; therefore, more neutral uranium must be processed. Processing more natural uranium to achieve a higher enrichment means increased output of depleted uranium. In this way, the higher enrichment of the mHTGR increases the energy-normalized mass of depleted uranium. The increased enrichment in the mHTGRs is critical to achieving the higher discharge burnups that drive the reduced spent nuclear fuel and high-level waste. The potential hazard and cost of disposal of spent nuclear fuel and high-level waste make the trade-off of increased depleted uranium for reduced spent nuclear fuel and high-level waste a positive choice.

Looking at the energy normalized mass of depleted uranium for the composite moderator mHTGRs shown in Figure 3.8, all four show reductions compared to the graphite reference mHTGR. The beryllium oxide case shows a 12.6 percent reduction in the energy-normalized mass of depleted uranium compared to the graphite reference, driven by a higher discharge burnup due to the higher moderating power of the beryllium over the graphite. The beryllium composite moderator shows a greater reduction of 30.2 percent compared to the graphite reference. This

increase compared to beryllium oxide is due to an even higher discharge burnup. The beryllium moderator achieves a higher discharge over the beryllium oxide due to the removal of the oxygen molecule bonded to the beryllium, as the beryllium is a better moderator than oxygen. The yttrium hydride moderator shows a 31.8 percent reduction compared to the graphite reference. This reduction is only slightly better compared to the beryllium oxide. The difference is again caused by increased discharge burnup in the yttrium case over the beryllium oxide. Still, it is much less significant than the change from the beryllium oxide to the beryllium case. The hydrogen molecules in the yttrium hydride have higher moderating power than the beryllium in the beryllium moderator, and with 1.9 hydrogen per yttrium, the hydrogen is also more abundant. Therefore,, the initial expectation would be for the yttrium hydride to showshow a significant increase in discharge burnup and, therefore,a significant decrease in the energy-normalized mass of depleted uranium. However, the decrease in the energy-normalized mass of depleted uranium between the beryllium and the yttrium cases is less than 2 percent. The yttrium in the yttrium composite moderator causes this limited reduction. Yttrium has a large absorption cross-section. Because of this large absorption cross-section, while the hydrogen atoms in the yttrium composite do slow more neutrons to thermal energies better than the beryllium in the beryllium case, more neutrons are absorbed outside the fuel and do not cause additional fissions. For this reason, the yttrium moderator sees only a slight benefit compared to the beryllium case for the energy-normalized mass of depleted uranium. Looking at the energy-normalized mass of depleted uranium for the zirconium-based composite moderator, a 45.0 percent reduction is observed compared to the graphite reference. This is a significant reduction compared to the 31.8 percent improvement in the yttrium composite moderator. While the zirconium composite moderator has fewer hydrogen atoms per molecule at 1.6 compared to

the yttrium composite moderator's 1.9, the zirconium does not have a high neutron absorption cross-section. The neutrons lost to parasitic absorption in the yttrium are greater than the reduced moderating power of fewer hydrogen atoms in the zirconium. Therefore, the zirconium composite moderator reactor has a higher discharge burnup, driving a lower energy-normalized mass of depleted uranium. The zirconium-based composite moderator has the lowest energy-normalized mass of depleted uranium of the mHTGR designs.

Comparing the energy-normalized mass of spent nuclear fuel and high-level waste in Figure 3.6 and the energy-normalized mass of depleted uranium seen in Figure 3.8, it is seen that the percent reduction in each composite moderator compared to the graphite reference is the same. This same percent reduction is due to both values being dependent only on the discharge burnup of the reactor fuel. Thus, the percent reduction in both the energy-normalized mass of spent nuclear fuel and high-level waste and the energy-normalized mass of depleted uranium are equivalent to the increase in discharge burnup achieved in the composite moderators. The difference between the energy-normalized mass of spent nuclear fuel and high-level waste and the energy-normalized mass of depleted uranium in the LWR, SMR, and the mHTGRs is not dependent only on discharge burnup. The discharge burnup-only trend does not extend to the LWR and SMR due to the LWR and SMR having different discharge burnups and thermal and electrical efficiencies. The fuel enrichment and thermal to electrical efficiencies in all five mHTGRs are constant.

Due to the higher enrichment driving increased depleted uranium production per unit of energy generated, all the mHTGRs show increased mass of depleted uranium per unit of energy generated compared to the LWR and SMR. However, the zirconium composite moderator with a 45.0 percent reduction compared to the graphite reference is close to the value seen in the SMR. Overall, the composite moderators produce

more depleted uranium per unit of energy, generating a large reduction in the energy-normalized mass of spent nuclear fuel and high-level waste seen when comparing the composite moderators to the LWR and SMR, Figure 3.6, mean that overall the composite moderators offer significant reductions in nuclear waste disposal cost and hazards with the zirconium case performing the best.

Combining the results of the three waste metric calculations, the mass of spent nuclear fuel and high-level waste, the mass of depleted uranium, and the volume of low-level waste all per unit of energy generated and seen in Figures 3.6, 3.8, and 3.7 the composite moderator perform as intended and reduce the nuclear waste impact. The most important of the three metrics is the energy-normalized mass of spent nuclear fuel and high-level waste seen in Figure 3.6; here, all the mHTGRs show excellent reductions compared to the LWR and SMR, and the composite moderators show further reductions compared to the state of the art graphite reference. The next most impact metric is the volume of low-level waste per unit of energy generated, shown in Figure 3.7. In this case, the composite moderators show results close to those of the LWR and SMR. This result is good considering the smaller size and higher enrichment of the mHTGRs. Additionally, the composite moderators significantly improve compared to the graphite state-of-the-art design. Finally, the mass of depleted uranium per unit of energy generated was calculated for each reactor design and shown in Figure 3.8. This metric is the least impact of the nuclear waste metrics as the potential radiation hazed from depleted uranium is minimal. In this case, the composite moderators showed reductions compared to the state-of-the-art graphite but increased energy-normalized mass of depleted uranium compared to the LWR and SMR. However, in the far greater cost and hazard of the spent nuclear fuel and high-level waste, an increase in depleted uranium for the trade-off of reduced spent nuclear fuel and high-level waste is well worth it.

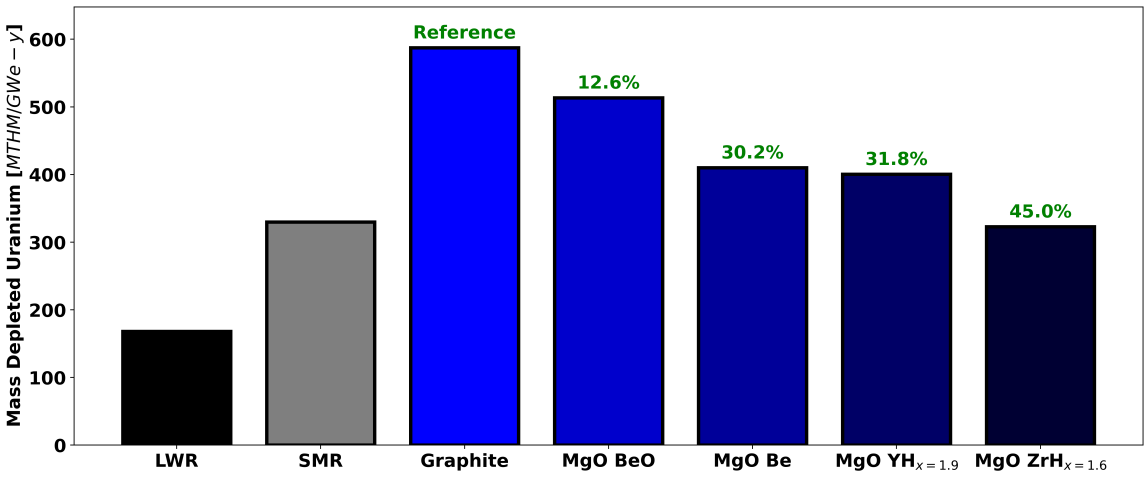

Figure 3.8: Energy normalized mass of depleted uranium for large-scale LWR, SMR, graphite micro-prismatic reference and prismatic IMF fuel concepts

Overall, the composite moderators show excellent improvement in nuclear waste production compared to a state-of-the-art graphite mHTGR and good improvement compared to current light water technologies.

3.3 Environmental Impact

The next set of metrics to be evaluated was the reactor operation's impact on the environment. To quantify this impact, several values were calculated: the mass of natural uranium used, the mass of carbon dioxide produced, the land used, and the volume of water used per unit of energy generated. The first metric calculated was the mass of natural uranium per unit of energy generated, shown in Figure 3.9. In Figure **??**, the advanced moderator mHTGR designs are compared to a state-of-the-art graphite design, a light water SMR, and an LWR reactor design. The graphite reference mHTGR uses more natural uranium per unit of energy generated compared to both the LWR and SMR and the higher fuel enrichment in the mHTGR designs causes this increase. More uranium 235 is needed in the fuel to achieve a higher enrichment since the amount of uranium 235 in natural and depleted uranium is constant. The only way to get a higher enrichment is to use more natural uranium and dispose of more depleted uranium. The higher enrichment is necessary to achieve higher discharge burnups, particularly in the smaller cores of micro-reactors due to higher leakage compared to large LWRs. Looking at the composite moderator materials compared to the graphite reference, we see reductions in the mass of natural uranium per unit of energy generated. The beryllium oxide case sees a 12.6 percent reduction; the beryllium shows a 30.2 percent reduction, the yttrium hydride a 31.8 percent reduction, and the zirconium hydride a 45.0 percent reduction to the mass

of natural uranium used per unit of energy generated. The reductions seen using the composite moderators are driven by the increased burnup in the composite moderator designs compared to the graphite reference case. The fuel is burned to a higher level with higher discharge burnup, so more power is generated with the same fuel mass and, therefore, the same natural uranium mass. Overall, the composite moderator designs are lower compared to the graphite reference but are higher than an LWR design and similar to an SMR design. The decreases in nuclear waste and the smaller package make the composite moderator mHTGR an appealing option.

The next metric evaluated was the mass of carbon dioxide produced across the fuel cycle per unit of energy generated. Carbon dioxide is not released during the reactor operation but is produced in other fuel cycle stages. Looking at Figure 3.10, the comparison of the mass of carbon dioxide produced per unit of energy generated for the composite moderators the reference graphite case and an SMR and LWR design. A similar trend in the case of natural uranium is seen where the graphite reference produces more carbon dioxide compared to the LWR and SMR, and the composite moderators show good reductions compared to the graphite reference. The beryllium oxide produces a 10.9 percent reduction, the beryllium sees a 26.2 percent reduction, the yttrium hydride shows a 27.6 percent reduction, and the zirconium hydride produces a 39.0 percent reduction. The increase in the carbon dioxide for the mHTGR is primarily driven by the high carbon dioxide production during the mining and milling process. Therefore, the increased use of natural uranium in the mHTGR designs drives increased carbon dioxide production. The mHTGRs produce carbon dioxide mass per unit of energy generated above that of a large LWR but is closer to the LWR value than was seen for the mass of natural uranium being used.

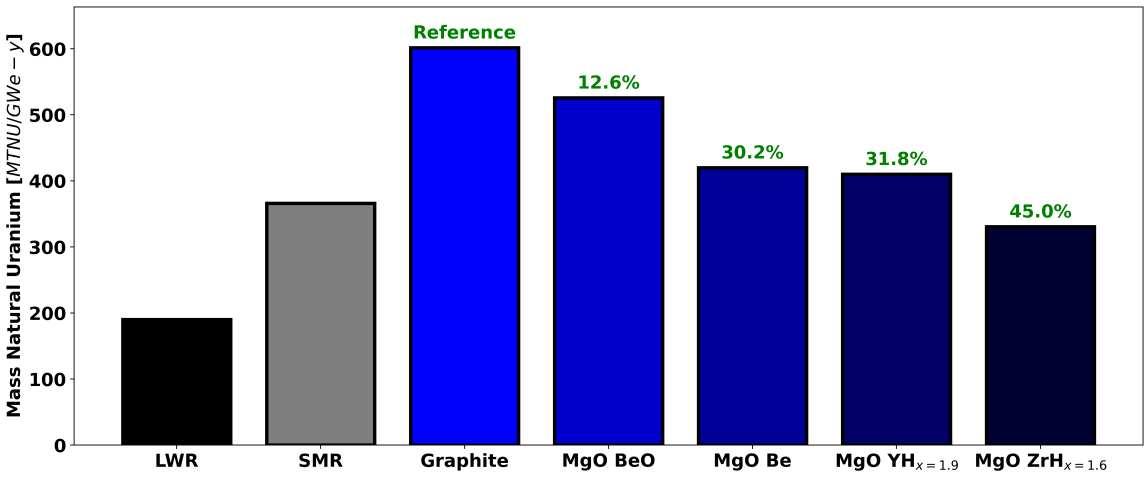

Figure 3.9: Energy normalized mass of natural uranium required for large-scale LWR, SMR, graphite micro-prismatic reference and prismatic IMF fuel concepts

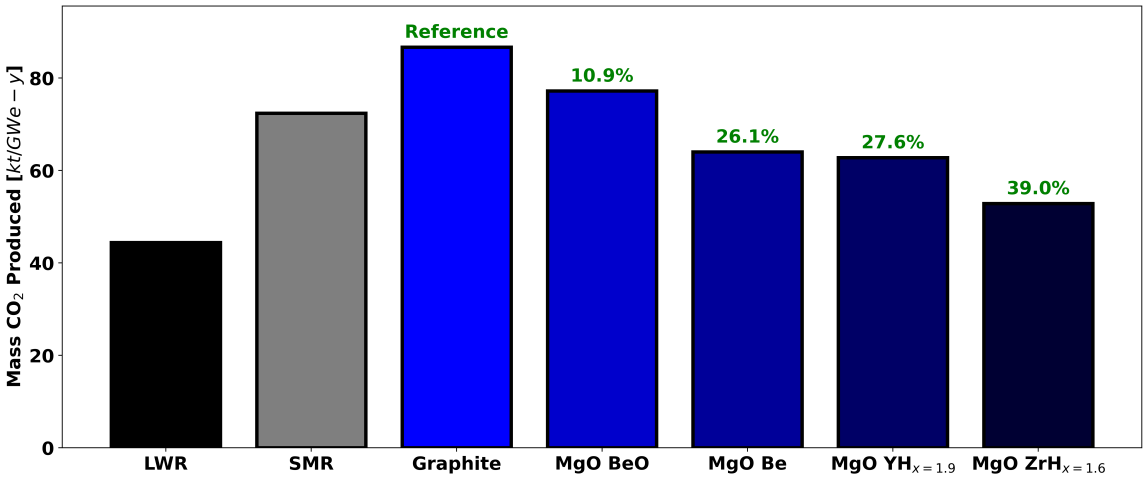

Figure 3.10: Energy normalized mass of carbon dioxide produced for large-scale LWR, SMR, graphite micro-prismatic reference and prismatic IMF fuel concepts

This result is due to the nuclear waste disposal process being another source of carbon dioxide production; therefore, the reduction in nuclear waste seen in the mHTGRs helps reduce the carbon dioxide mass being released. Another metric evaluated was the total land area used per unit of energy generated across the fuel cycles. Figure 3.11 shows the land area in square km per unit of energy generated for the graphite reference of the four composite moderators and the LWR and SMR reactors. As with the carbon dioxide and the mass of natural uranium, the graphite reference uses more land compared to the LWR and SMR, and the composite moderators show good reductions compared to the graphite reference. The composite moderators produced reductions of 9.83 percent for the beryllium oxide, 23.5 percent for the beryllium case, 24.8 percent for the yttrium hydride case, and 35.1 percent for the zirconium hydride case. As with the carbon dioxide case, the significant contributions to the land area come first from mining and milling and, secondly, from nuclear waste disposal. Therefore, the higher enrichment leads to an increased mass of natural uranium, increasing the land area required for mining. Conversely, the decrease in nuclear waste in the composite moderators leads to less nuclear waste, requiring a smaller land area to dispose of the waste. Overall, the composite moderators use more land area per unit of energy generated compared to an LWR but less compared to a state-of-the-art graphite mHTGR.

The last metric considered in the environmental impact calculations is the volume of water used per unit of energy generated in the reactor. Figure 3.12 shows the volume of water used per unit of energy generated for the LWR, SMR, graphite reference and the four composite moderator designs. As can be seen, there is less than a 2 percent difference across all seven reactor concepts. This lack of change in the volume of water used is due to the water calculation equation being dominated by the reactor operation term.

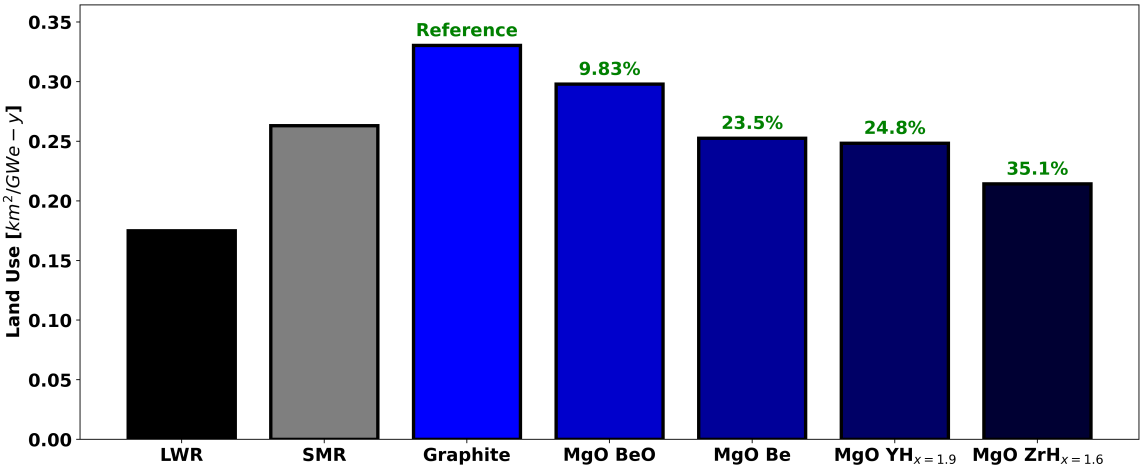

Figure 3.11: Energy normalized land area use for large-scale LWR, SMR, graphite micro-prismatic reference and prismatic IMF fuel concepts

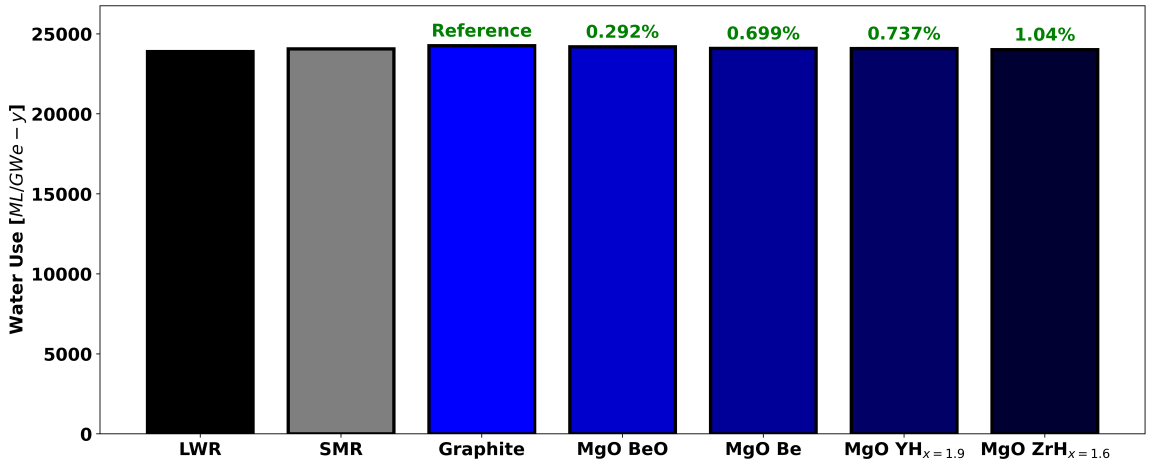

Figure 3.12: Energy normalized volume of water used for large-scale LWR, SMR, graphite micro-prismatic reference, and prismatic IMF fuel concepts

The reactor operation term at a set volume per unit energy used is constant and dominates the equation due to being the final heat sink of the reactor. For all the reactor concepts, the heat generated by fission heats the coolant; the coolant then goes through a steam generator to create steam; the steam drives a turbine to generate electricity and is then condensed back to water using an outside water source. This water source used to condense the water back to steam is the same volume per unit of energy, accounting for almost all the water used in the fuel cycle. Therefore, the total volume of water used does not significantly change across reactor concepts.// Overall, looking at the mass of natural uranium, the mass of carbon dioxide produced, the land area used, and the volume of water gives a good picture of the total environmental impact of the reactor concepts. The water volume was essentially constant across the reactor concepts. For the other metrics, the composite moderators consistently performed better than the state-of-the-art graphite reference but above that of the LWR case. As discussed previously, this outcome shows a trade-off between decreasing the spent nuclear fuel and the environmental impact. The high cost, danger, and potential hazard of nuclear waste make the slight environmental impact of significantly reducing the mass of nuclear waste an appealing trade-off.

3.4 Fuel Cost

Another metric calculated to evaluate the composite moderator design performance was the front-end fuel cycle cost. Figure 3.13 shows the front-end fuel cycle cost for the LWR, SMR, graphite reference, and composite moderator designs. Here the SMR is seen to have a far higher fuel cost compared to the LWR due to the high cost of advanced fuel forms. Similarly, the reference graphite case has a higher fuel cost due to the high cost of TRISO fuel fabrication. Table 2.7 shows the cost of TRISO fuel,

and Table 2.8 shows the cost of LWR fuel. These tables shown that the high cost of UN TRISO fuel is primarily due to the high fuel fabrication cost compared to that of LWRs. However, the high cost of TRISO fuel fabrication is mainly due to the novelty of the fuel type. As TRISO fuel becomes more common, the supply chain for TRISO fuel will be established, and the cost of TRISO fuel fabrication reduced. The cost of the composite moderators compared to the graphite reference case shows reductions for all moderators. The beryllium oxide case shows a 12.6% reduction; the beryllium case shows a 30.2% reduction, the yttrium hydride shows a 31.8% reduction, and the zirconium hydride shows an 45.0% decrease in the fuel cost per unit energy generated compared to the graphite reference case. Overall, the composite moderators show reduced front-end fuel cycle cost compared to the SMR reactor and the mHTGR graphite reference design but higher costs compared to traditional LWR reactors. This higher cost is due to the better-established supply chain for light-water reactor fuel than advanced reactor fuel concepts. Therefore, in the case of advanced reactors, the composite moderator reactors show sound fuel cost reduction.

3.5 Nuclear Waste Activity

Finally, the activity of the SNF&HLW at 100 and 10,000 years is a measure of the challenges to nuclear waste disposal. Figure 3.14 shows the activity of the LWR, the SMR, the graphite reference case, and the four composite moderator reactors. The graphite reference case and the composite moderators have activities below that of the LWR and SMR. The beryllium oxide reactor has 9.03 percent higher activity compared to the graphite reference case. The beryllium case sees a 1.68 percent increase in activity compared to the graphite reference case.

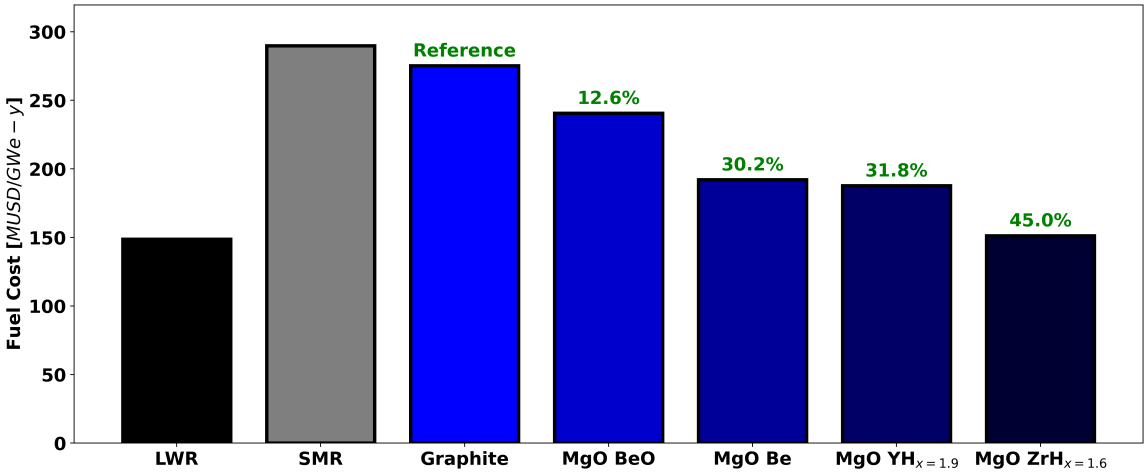

Figure 3.13: Energy normalized front end fuel cost for large-scale LWR, SMR, graphite micro-prismatic reference and prismatic IMF fuel concepts

The yttrium hydride case sees a 25.2 percent reduction in activity compared to the graphite reference case. The zirconium hydride has a 29.0% decrease in activity compared to the graphite reference case.

Figure 3.15 shows the activity after 100,000 years for the SNF&HLW for the LWR, SMR, graphite reference, and composite moderator designs. In this case, the graphite reference and the composite moderators are below the SMR value and close to or below that of the LWR. The beryllium oxide, beryllium, and yttrium hydride cases see increased reactivity compared to the graphite reference by 17.0, 5.25, and 4.03 percent, respectively. The zirconium hydride produces 19.5 percent less activity than the graphite reference case. Overall, the activity results at 100 and 100,000 years show that the SNF&HLW produced in the composite moderator mHTGR does not lead to increased challenges or costs compared to traditional light water reactor waste.

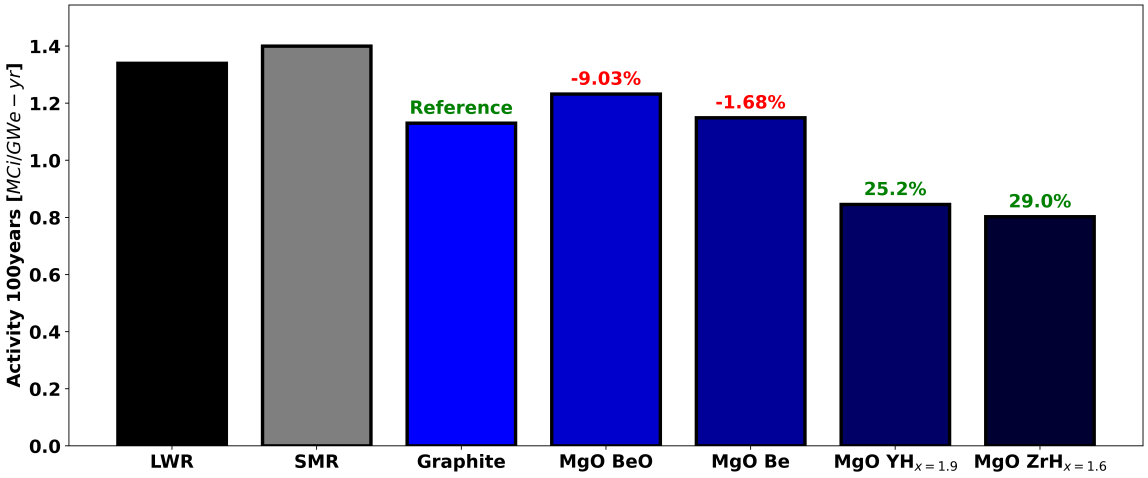

Figure 3.14: Energy normalized activity of SNF&HLW after 100 years for large-scale LWR, SMR, graphite micro-prismatic reference, and prismatic IMF fuel concepts

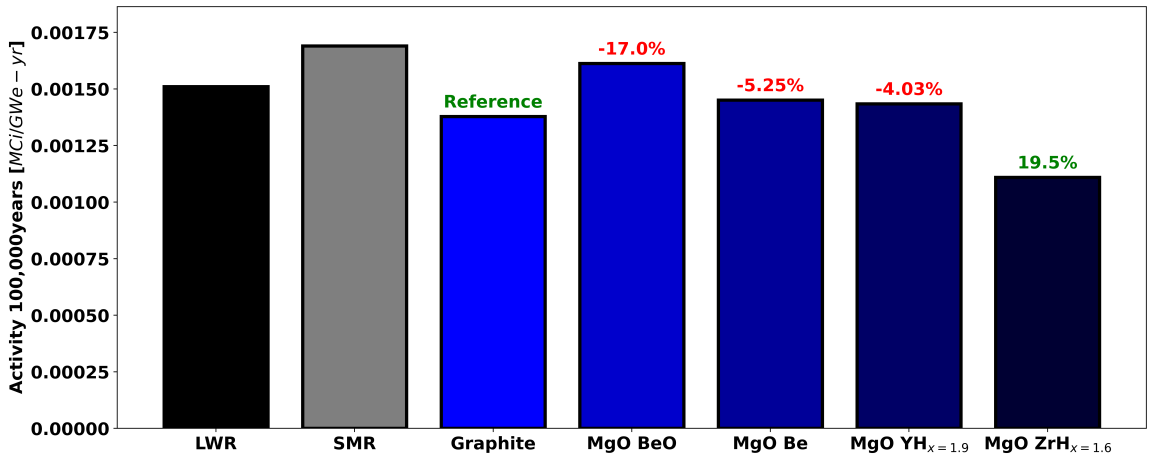

Figure 3.15: Energy normalized activity of SNF&HLW after 100,000 years for large-scale LWR, SMR, graphite micro-prismatic reference, and prismatic IMF fuel concepts

Chapter 4

Conclusions

This work explored two-phase composite moderators combined with IMF forms to improve critical metrics over the fuel cycle of a micro-HTGR. The IMF fuel employed MgO as a matrix material with four composite moderators considered within a prismatic architecture: $MgO - BeO$, $MgO - B\text{e}$, $MgO - YH_{x=1.9}$, and $MgO - ZrH_{x=1.6}$. The current state of the art for HTGRs is a graphite moderated reactor. As such, a graphite design was created within the same size constraints to serve as a reference case for the micro-reactor cases, producing the same thermal and electrical power as the IMF designs. With the basic geometry for the reactor set, unique optimal configurations for each moderator material were found by running optimization sweeps over the TRISO packing fraction and lattice pitch. In this way, the optimal fuel-to-moderator ratio to increase discharge burnup was identified. The designs were evaluated primarily for the mass of SNF&HLW produced per unit energy generated, which is directly driven by the discharge burnup achieved in the fuel and, therefore, used as the target of the optimization sweeps.

After the optimal configurations were identified, key metrics were evaluated and compared between each mHTGR moderator design, a reference graphite mHTGR,

and a reference LWR and SMR design from the literature. The advanced moderator mHTGRs all produced significantly reduced SNF&HLW per unit of energy generated when compared to the LWR and SMR. This reduction is beyond that of a graphite mHTGR, producing 12.6%, 30.2%, 31.8%, and 45.0% less for the beryllium oxide, beryllium, yttrium hydride, and zirconium hydride, respectively compared to the graphite design. This reduction trend continued for the volume of low-level waste, with the beryllium oxide, beryllium, yttrium hydride, and zirconium hydride producing 31.4%, 37.9%, 38.5%, and 43.5% reductions respectively compared to the graphite reference case. Similarly, for the mass of depleted uranium per unit of energy generated, the composite moderators saw reductions of 12.6%, 30.2%, 31.8%, and 45.0% for the beryllium oxide, beryllium, yttrium hydride, and zirconium hydride respectively compared to the graphite reference.

The environmental impact of the composite moderators was then evaluated by calculating the mass of natural uranium, the mass of carbon dioxide, land area used, and water volume used per unit of energy generated. The composite moderators continued to produce improvements over the graphite reference case for the environmental metrics. For the mass of natural uranium per unit of energy generated, the composite moderators produced a 12.6%, 30.2%, 31.8%, and 45.0% reduction for beryllium oxide, beryllium, yttrium hydride, and zirconium hydride respectively compared to the graphite reference. For the energy normalized mass of carbon dioxide, the beryllium oxide, beryllium, yttrium hydride, and zirconium hydride moderators produced reductions of 10.9%, 26.1%, 27.6%, and 39.0% reductions respectively compared to the graphite moderator. Looking at the land area per unit energy generated, the composite moderators show reductions of 9.83%, 23.5%, 24.8%, and 35.1% for beryllium oxide, beryllium, yttrium hydride, and zirconium hydride respectively compared to the graphite reference case. Regarding

the volume of water used per unit of energy generated, the composite moderators had a minor impact, reducing the value by less than 2 percent in all cases compared to the graphite reference.

The front-end fuel cycle cost and the activity level of the SNF&HLW at 100 and 100,000 years were also evaluated. In the case of the fuel cost, the composite moderators reduced the cost by 12.6% for the beryllium oxide case, 30.2% for the beryllium case, 31.8% for the yttrium hydride case, and 45.0% for the zirconium hydride case all being compared to the graphite reference. For the activity at 100 years per unit of energy generated, the beryllium oxide produced a 9.03% increase in activity, the beryllium a 1.68% increase in activity, the yttrium hydride a 25.2% reduction in activity, and the zirconium hydride a 29.0% reduction in activity all being compared to the graphite reference case. While some cases did see increases rather than reductions, the activity of the SNF&HLW after 100 years is within the same range as the reference and does not present increased disposal cost or risk. A similar case was seen at 100,000 years, where some of the composite moderator designs saw an increase in activity and others saw a decrease. Still, across all designs, the activity after 100,000 years did not increase the risk or cost of disposal. Specifically, the composite moderator's increases of 17.0%, 5.25%, and 4.03% for the beryllium oxide, beryllium, and yttrium hydride, respectively and a 19.5% reduction for the zirconium hydride case compared to the graphite reference.

The composite moderator mHTGR designs were also compared to an LWR and SMR for each of the calculated metrics. For the nuclear waste metrics mass of SNF&HLW and the volume of low-level waste, the composite moderators show good reduction compared to the LWR and SMR. For the mass of depleted uranium and the environmental impact metrics, the composite moderators show increases compared to the LWR and SMR due to the higher enrichment in the meter. Overall, the slight

increase in other metrics for the composite moderator mHTGRs is a drawback that is more than accounted for by the significant reduction in nuclear waste. The front-end fuel cycle cost was higher in the mHTGRs compared to the LWR and the SMR; however, this is primarily due to the high fabrication cost of TRISO, which would be expected to be reduced as supply chains are built up with TRISO fuel being used in reactors. For the activity of the SNF&HLW after 100 and 100,000 years, the composite moderators and LWr and SMR have comparable results. Overall, the utilization of composite moderator IMF HTGRs leads to significant reductions in the mass of SNF&HLW and the volume of LLW produced per unit of energy generated with comparable environmental impact, fuel cost, and spent fuel activity to traditional LWR technologies.

Bibliography

[1] Nicholas Apergis, James E Payne, Kojo Menyah, and Yemane Wolde-Rufael. On the causal dynamics between emissions, nuclear energy, renewable energy, and economic growth. *Ecological Economics*, 69(11):2255–2260, 2010. 6

[2] World Nuclear Association. Small nuclear power reactors. Available at https://world-nuclear.org/information library/nuclear-fuel-cycle/nuclear-power-reactors/small-nuclear-power-reactors. 1

[3] Jungho Baek. A panel cointegration analysis of co2 emissions, nuclear energy and income in major nuclear generating countries. *Applied Energy*, 145:133–138, 2015. 6

[4] H. L. Brey. Fort st. vrain operations and future. 16(1):47–58. 5

[5] N. R. Brown, J. J. Powers, B. Feng, F. Heidet, N. E. Stauff, G. Zhang, M. Todosow, A. Worrall, J. C. Gehin, T. K. Kim, and T. A. Taiwo. Sustainable thorium nuclear fuel cycles: A comparison of intermediate and fast neutron spectrum systems. 289:252–265. 20

[6] Nicholas R Brown. Fuel cycle performance of thermal spectrum small modular reactors. 20

[7] Nicholas R. Brown. A review of in-pile fuel safety tests of TRISO fuel forms and future testing opportunities in non-HTGR applications. 534:152139. 13

[8] Nicholas R. Brown, Richard Hernandez, and Andrew T. Nelson. High volume packing fraction TRISO-based fuel in light water reactors. 146:104151. 20

[9] Nicholas R. Brown, Jeffrey J. Powers, Michael Todosow, Massimiliano Fratoni, Hans Ludewig, Eva E. Sunny, Gilad Raitses, and Arnold Aronson. Thorium fuel cycles with externally driven systems. 194(2):233–251. Publisher: Taylor & Francis _eprint: https://doi.org/10.13182/NT15-40. 20

[10] Nicholas R. Brown and Shripad T. Revankar. An endothermic chemical process facility coupled to a high temperature reactor. part II: Transient simulation of accident scenarios within the chemical plant. 246:266–276. 6

[11] Nicholas R. Brown, Volkan Seker, Shripad T. Revankar, and Thomas J. Downar. An endothermic chemical process facility coupled to a high temperature reactor. part i: Proposed accident scenarios within the chemical plant. 246:256–265. 6

[12] Nicholas R. Brown, Andrew Worrall, and Michael Todosow. Impact of thermal spectrum small modular reactors on performance of once-through nuclear fuel cycles with low-enriched uranium. 101:166–173. 20, 59, 63, 64

[13] Timothy D. Burchell and Lance L. Snead. The effect of neutron irradiation damage on the properties of grade NBG-10 graphite. 371(1):18–27. 14

[14] Joseph R. Burns, Richard Hernandez, Kurt A. Terrani, Andrew T. Nelson, and Nicholas R. Brown. Reactor and fuel cycle performance of light water reactor fuel with 235u enrichments above 5%. 142:107423. 20

[15] Donald E Carlson and Sydney J Ball. Perspectives on understanding and verifying the safety terrain of modular high temperature gas-cooled reactors. *Nuclear Engineering and Design*, 306:117–123, 2016. 4

[16] Liam Carlson, James Miller, and Zeyun Wu. Implications of haleu fuel on the design of smrs and micro-reactors. *Nuclear Engineering and Design*, 389:111648, 2022. 1, 2

[17] N Chauvin, T Albiol, R Mazoyer, J Noirot, D Lespiaux, J. C Dumas, C Weinberg, J. C Ménard, and J. P Ottaviani. In-pile studies of inert matrices with emphasis on magnesia and magnesium aluminate spinel. 274(1):91–97. 18

[18] Bin Cheng, Edward M. Duchnowski, David J. Sprouster, Lance L. Snead, Nicholas R. Brown, and Jason R. Trelewicz. Ceramic composite moderators as replacements for graphite in high temperature microreactors. 563:153591. 18

[19] F. W. Clinard, G. F. Hurley, and L. W. Hobbs. Neutron irradiation damage in MgO, al2o3 and MgAl2o4 ceramics. 108-109:655–670. 18

[20] Paul A Demkowicz, Bing Liu, and John D Hunn. Coated particle fuel: Historical perspectives and current progress. *Journal of Nuclear Materials*, 515:434–450, 2019. xi, 12, 13, 15, 16

[21] Edward M. Duchnowski, Robert F. Kile, Kenny Bott, Lance L. Snead, Jason R. Trelewicz, and Nicholas R. Brown. Pre-conceptual high temperature gas-cooled microreactor design utilizing two-phase composite moderators. part i: Microreactor design and reactor performance. 149:104257. x, xi, 18, 21, 22, 24, 26, 27

[22] James L Everett III and Edward J Kohler. Peach bottom unit no. 1: A high performance helium cooled nuclear power plant. *Annals of Nuclear Energy*, 5(8-10):321–335, 1978. 12

[23] Nathan Michael George, Ivan Maldonado, Kurt Terrani, Andrew Godfrey, Jess Gehin, and Jeff Powers. Neutronics studies of uranium-bearing fully ceramic microencapsulated fuel for pressurized water reactors. 188(3):238–251. Publisher: Taylor & Francis _eprint: https://doi.org/10.13182/NT14-3. 13

[24] Carlotta G Ghezzi and Nicholas R Brown. TRISO burnup-dependent failure analysis in FHRs using BISON. 586:154651. Publisher: Elsevier. 13

[25] WV Goeddel. Coated-particle fuels in high-temperature reactors: a summary of current applications. *Nuclear Applications*, 3(10):599–614, 1967. 12

[26] A. L. Habush and A. M. Harris. 330-MW(e) fort st. vrain high-temperature gas-cooled reactor. 7(4):312–321. xi, 5, 8, 12, 14, 21

[27] Florent Heidet, Nicholas R. Brown, and Malek Haj Tahar. Accelerator–reactor coupling for energy production in advanced nuclear fuel cycles. 08:99–114. Publisher: World Scientific Publishing Co. 20

[28] M. C. R. Heijna, S. de Groot, and J. A. Vreeling. Comparison of irradiation behaviour of HTR graphite grades. 492:148–156. 14

[29] Richard Hernandez and Nicholas R. Brown. Potential fuel cycle performance of floating small modular light water reactors of russian origin. 144:107555. 20

[30] Richard Hernandez, Michael Todosow, and Nicholas R. Brown. Micro heat pipe nuclear reactor concepts: Analysis of fuel cycle performance and environmental impacts. 126:419–426. 20

[31] Shouyin Hu, Ruipian Wang, and Zuying Gao. Transient tests on blower trip and rod removal at the HTR-10. 236(5):677–680. 5

[32] Hiroki Iwata, Keisuke Okada, and Sovannroeun Samreth. Empirical study on the environmental kuznets curve for co2 in france: the role of nuclear energy. *Energy policy*, 38(8):4057–4063, 2010. 6

[33] K Jenni. Nuclear fuel cycle evaluation and screening–final report. 2014. x, xi, 20, 28, 29, 30, 31, 32, 33, 34, 35, 37, 39, 40

[34] Veronica Karriem, Edward M. Duchnowski, Bin Cheng, Lance L. Snead, Jason R. Trelewicz, and Nicholas R. Brown. Reactor performance and safety characteristics of beryllium-based composite moderators as replacements for graphite in mHTGRs. 208(7):1102–1113. Publisher: Taylor & Francis _eprint: https://doi.org/10.1080/00295450.2021.2011573. 18

[35] B.T. Kelly. *Physics of graphite*. Applied Science. INIS Reference Number: 13661340. 14

[36] Pauli Lappi and Jussi Lintunen. From cradle to grave? on optimal nuclear waste disposal. 103:105556. 12

[37] Ruihan Li, Zhaoyuan Liu, Zhiyuan Feng, Jingang Liang, and Liguo Zhang. High-fidelity MC-DEM modeling and uncertainty analysis of HTR-PM first criticality. 9. Publisher: Frontiers. 12, 14

[38] Cihang Lu and Nicholas R. Brown. Fully ceramic microencapsulated fuel in prismatic high-temperature gas-cooled reactors: Design basis accidents and fuel cycle cost. 347:108–121. x, 14, 38

[39] Cihang Lu, Briana D Hiscox, Kurt A Terrani, and Nicholas R Brown. Fully ceramic microencapsulated fuel in prismatic high temperature gas-cooled reactors: analysis of reactor performance and safety characteristics. 114:277–287. Publisher: Elsevier. 14, 18

[40] Jacob W. McMurray, Terrence B. Lindemer, Nicholas R. Brown, Tyler J. Reif, Robert N. Morris, and John D. Hunn. Determining the minimum required uranium carbide content for HTGR UCO fuel kernels. 104:237–242. 13

[41] Kojo Menyah and Yemane Wolde-Rufael. Co2 emissions, nuclear energy, renewable energy and economic growth in the us. *Energy Policy*, 38(6):2911–2915, 2010. The Role of Trust in Managing Uncertainties in the Transition to a Sustainable Energy Economy, Special Section with Regular Papers. 6

[42] David Petti, Robert Hill, J Gehin, Hans Gougar, Gerhard Strydom, T O'Connor, F Heidet, Jim Kinsey, Chris Grandy, A Qualls, et al. A summary of the department of energy's advanced demonstration and test reactor options study. *Nuclear Technology*, 199(2):111–128, 2017. 4, 6

[43] MST Price. The dragon project origins, achievements and legacies. *Nuclear engineering and design*, 251:60–68, 2012. xi, 7, 12

[44] R. J. Price. Effects of fast-neutron irradiation on pyrolytic silicon carbide. 33(1):17–22. 14

[45] M. V. Ramana. The checkered operational history of high-temperature gas-cooled reactors. 72(3):171–179. Publisher: Routledge _eprint: https://doi.org/10.1080/00963402.2016.1170395. 5

[46] Sirazam Sadekin, Sayma Zaman, Mahjabin Mahfuz, and Rashid Sarkar. Nuclear power as foundation of a clean energy future: A review. 160:513–518. xi, 6, 10

[47] Hiroyuki Sato and Xing L. Yan. Study of an HTGR and renewable energy hybrid system for grid stability. 343:178–186. 6

[48] Fiona Caroline Saunders and Ellen A Townsend. Delivering new nuclear projects: a megaprojects perspective. *International Journal of Managing Projects in Business*, 12(1):144–160, 2019. 2

[49] L. L. Snead and T. D. Burchell. Thermal conductivity degradation of graphites due to nuetron irradiation at low temperature. 224(3):222–229. 14

[50] L. L. Snead, T. D. Burchell, and Y. Katoh. Swelling of nuclear graphite and high quality carbon fiber composite under very high irradiation temperature. 381(1):55–61. 14

[51] Lance L. Snead, Takashi Nozawa, Yutai Katoh, Thak-Sang Byun, Sosuke Kondo, and David A. Petti. Handbook of SiC properties for fuel performance modeling. 371(1):329–377. 14

[52] Lance L Snead, David Sprouster, Bin Cheng, Nick Brown, Caen Ang, Edward M Duchnowski, Xunxiang Hu, and Jason Trelewicz. Development and potential of composite moderators for elevated temperature nuclear applications. 10(1):9–32. Publisher: Taylor & Francis _eprint: https://doi.org/10.1080/21870764.2021.1993592. xi, 18, 19

[53] OM Stansfield. Evolution of htgr coated particle fuel design. *Energy*, 16(1-2):33–45, 1991. 13

[54] K. A. Terrani, J. O. Kiggans, Y. Katoh, K. Shimoda, F. C. Montgomery, B. L. Armstrong, C. M. Parish, T. Hinoki, J. D. Hunn, and L. L. Snead. Fabrication and characterization of fully ceramic microencapsulated fuels. 426(1):268–276. 14

[55] Kurt A. Terrani, Caen Ang, Lance L. Snead, and Yutai Katoh. Irradiation stability and thermo-mechanical properties of NITE-SiC irradiated to 10 dpa. 499:242–247. x, 14, 23

[56] Kurt A. Terrani, Brian C. Jolly, and Jason M. Harp. Uranium nitride tristructural-isotropic fuel particle. 531:152034. xi, 13, 14, 17

[57] Raffaella Testoni, Andrea Bersano, and Stefano Segantin. Review of nuclear microreactors: Status, potentialities and challenges. *Progress in Nuclear Energy*, 138:103822, 2021. xi, 2, 3, 4, 6

[58] Elizabeth Wachs and Bernard Engel. Land use for united states power generation: A critical review of existing metrics with suggestions for going forward. *Renewable and Sustainable Energy Reviews*, 143:110911, 2021. xi, 6, 11

[59] Ben Wealer, Victoria Czempinski, Christian von Hirschhausen, and Sebastian Wegel. Nuclear energy policy in the united states: Between rocks and hard places. In *IAEE Energy Forum Second Quarter*, pages 67–78, 2017. 12

[60] Zongxin Wu, Dengcai Lin, and Daxin Zhong. The design features of the HTR-10. 218(1):25–32. xi, 5, 9, 12, 14

Vita

Donald Lukas Doyle graduated from Texas A&M University with a Bachelor of Science in Nuclear Engineering In May of 2022. Donald started attending The University of Tennessee, Knoxville in August of 2022 to peruse a Master of Science and Doctorate of Philosophy in Nuclear Engineering. Donald has presented work at the American Nuclear Society Winter meeting in November of 2023 and has a peer reviewed journal article in Nuclear Engineering and Design currently under review for publication.